Stellar Atmosphere Modeling
ASP Conference Series, Vol. 288, 2003
I. Hubeny, D. Mihalas, & K. Werner, eds.

The Generation and Transfer of Polarized Radiation in Stellar Atmospheres

Javier Trujillo Bueno[1]

Instituto de Astrofísica de Canarias, 38200 La Laguna, Tenerife, Spain

Abstract. This paper addresses the modeling issue of spectral line polarization in stellar atmospheres, taking into account scattering processes and the Hanle and Zeeman effects in two-level and multilevel atomic models, and with the statistical equilibrium and radiative transfer equations formulated within the framework of the quantum theory of polarization. After arguing why this research field is of real astrophysical interest, the basic equations and anisotropic pumping mechanisms are reviewed. Finally, it is shown how to solve efficiently a variety of polarization transfer problems via the application of fast iterative methods and accurate formal solvers of the Stokes vector transfer equation.

1. Introduction

Most observational work in astrophysics has so far been carried out mainly on the basis of the intensity of the radiation received from the object observed as a function of wavelength. However, an important but frequently overlooked aspect of electromagnetic radiation is its state of polarization, which is related to the orientation of the electric field of the wave. The state of polarization of a quasi-monochromatic beam of electromagnetic radiation can be conveniently characterized in terms of four quantities that can be measured by furnishing our telescopes with a polarimeter. These observables are the four Stokes parameters (I, Q, U, V) which were formulated by Sir George Stokes in 1852 and introduced into astrophysics by the Nobel laureate Subrahmanyan Chandrasekhar in 1946. The Stokes $I(\lambda)$ profile represents the *intensity* as a function of wavelength, Stokes $Q(\lambda)$ the *intensity difference* between vertical and horizontal linear polarization, Stokes $U(\lambda)$ the *intensity difference* between linear polarization at $+45°$ and $-45°$, while Stokes $V(\lambda)$ the *intensity difference* between right-handed and left-handed circular polarization (cf. Born & Wolf 1994). Note that the definition of the Stokes Q and U parameters requires to choose first a reference direction for $Q > 0$ in the plane perpendicular to the direction of propagation.

There are numerous physical mechanisms that can generate polarized radiation (e.g. Rybicki & Lightman 1979; Landi Degl'Innocenti 2002). In stellar atmospheres, the most important mechanisms that induce (and modify) polarization signatures in spectral lines are the Zeeman effect, anisotropic radiation

[1]Consejo Superior de Investigaciones Científicas, Spain.

pumping and the Hanle effect (e.g. Trujillo Bueno 2001). All these physical mechanisms leave their 'fingerprints' in the polarization of the electromagnetic radiation that we collect with our increasingly large telescopes (see *Astrophysical Spectropolarimetry*, edited by Trujillo Bueno, Moreno-Insertis & Sánchez 2002*a*). The interesting point is that the development of diagnostic techniques that combine the Hanle and Zeeman effects in suitably chosen spectral lines may allow us to investigate the strength and topology of stellar magnetic fields in a parameter domain which ranges from at least milligauss till thousands of gauss. Moreover, the observation and rigorous physical interpretation of polarized radiation may also help us to verify the geometry of the astrophysical system under investigation, even without being possible to resolve it spatially[2]. Such remote sensing techniques are based on the theory and numerical modeling of the generation and transfer of polarized radiation in magnetized plasmas.

In my opinion, at present the most suitable theoretical framework for modeling polarization signals in spectral lines is the quantum theory of line formation, as developed by Landi Degl'Innocenti (1983). In this theory, the excitation state of the atomic (or molecular) system is described by the *diagonal* and *non-diagonal* elements of the atomic density matrix, which provide information on the *population imbalances* and *quantum coherences* (or interferences) between the magnetic sublevels, respectively. Similarly, the symmetry properties of the radiation field are described by 9 tensors which quantify the mean intensity, the 'degree of anisotropy', the degree of breaking of the axial symmetry, etc. (see the review by Trujillo Bueno 2001). This QED theory is based on the Markovian assumption of complete frequency redistribution (see a critical review in Trujillo Bueno 1990). For problems where the only significant coherences are those between the sublevels pertaining to each degenerate level, it provides a physically consistent description of scattering phenomena *if* the spectrum of the pumping radiation is flat across a frequency range wider than both the Larmor frequency (ν_L) and the inverse lifetime of the levels (see Landi Degl'Innocenti *et al.* 1997). As discussed by Trujillo Bueno & Manso Sainz (2002), this turns out to be a sufficiently good approximation for modeling the observed polarization signatures in a variety of solar spectral lines (e.g. the Ca II IR triplet, the Mg I *b* lines, the He I 10830 multiplet, the O I triplet at 777 nm, etc.) [3].

The logical structure of this article is the following. Sections 2 and 3 consider the iterative methods we had developed for the efficient solution of 'unpolarized' RT problems. The next four sections introduce the basic physical mechanisms and the general equations, including the development of two new formal solvers of the Stokes-vector transfer equation. Section 8 focuses on the iterative solution of *linear* polarization transfer problems, assuming a two-level atomic model without ground-level polarization. We consider the following cases: resonance

[2]Completely unpolarized radiation can be expected only from a perfectly symmetric object.

[3]Although much theoretical work remains to be done, the first steps towards the generalization of this density matrix theory to partial frequency redistribution (PRD) have already been taken (e.g. Bommier 1997*a*, *b*; Landi Degl'Innocenti et al. 1997). The key issue now is to derive, from the first principles of QED, a consistent set of equations capable of describing scattering polarization in spectral lines taking fully into account the presence of lower-level atomic polarization in all the lines of the assumed atomic model.

line polarization, the Hanle effect and the Zeeman effect. Section 9 concerns the iterative solution of the general (*non-linear*) problem where we allow for the possibility of lower-level polarization in two-level and multilevel atomic systems, in the absence and in the presence of weak magnetic fields. Finally, section 10 gives some concluding remarks.

2. The standard Non-LTE problem

The standard Non-LTE problem (e.g. Mihalas 1978) consists in calculating the atomic (or molecular) level *populations* that are consistent with the *intensity* of the radiation field generated within any given stellar atmospheric model. This requires solving jointly the radiative transfer (RT) equations for the specific *intensity* and the rate and conservation equations for the level *populations*. Note that each level of total angular momentum J has associated with it one single unknown: its overall population n_J.

The combination of such equations leads to a coupled system of the form

$$\mathbf{A}\,\mathbf{x} = \mathbf{b}, \tag{1}$$

where $\mathbf{A}$ is an operator whose coefficients depend on collisional and radiative rates, $\mathbf{b}$ is a known vector and $\mathbf{x}$ is the unknown vector formed by the populations of the assumed atomic or molecular model at all the spatial grid points. In general, the standard Non-LTE problem is *non-linear*, i.e. the elements of the operator $\mathbf{A}$ depend on $\mathbf{x}$. This is because the radiative rates that are proportional to the radiation field intensity (i.e. the *transfer* and *relaxation* rates due to absorption and stimulated emission processes) depend implicitly on the level populations via the radiative transfer equations. Because of this non-linearity, iterative algorithms are necessary to solve Eqs. (1). Here, at each iterative step, one has to manage to set up a suitable linear system of equations whose solution leads to approximate corrections to the unknowns. The paper by Socas-Navarro & Trujillo Bueno (1997) clarifies why the preconditioning strategy of Rybicki & Hummer (1991; 1992) is the most suitable one for achieving easily the required linearity of the statistical equilibrium (SE) equations at each iterative step, independently of the fact that the *linearization* and *preconditioning* techniques may lead to similar sets of linearized equations if the same information is taken into account.

Finally, note that iterative methods that require the construction and inversion of large matrices at each iterative step are of little practical interest. It was therefore imperative to develop novel RT methods where everything goes as simply as in the Λ-iteration scheme, but for which the convergence rate is *extremely* high (see the reviews by Auer and by Hubeny in these proceedings).

3. Iterative methods for radiative transfer applications

The essential ideas behind the iterative schemes on which our Non-LTE multilevel transfer codes are based on can be easily understood by considering the 'simplest' Non-LTE problem: the coherent scattering case with source function

$$S = (1-\epsilon)J + \epsilon B, \tag{2}$$

where ϵ is the Non-LTE parameter, J the mean intensity and B the Planck function. Note that the mean intensity at the spatial grid point 'i' is the angular average of incoming ('*in*') and outgoing ('*out*') contributions of the specific intensity.

The well-known $\Lambda-$iteration scheme is to do the following in order to obtain the 'new' estimate of the source function at each spatial grid-point 'i':

$$S_i^{\rm new} = (1-\epsilon)J_i^{\rm old} + \epsilon B_i, \tag{3}$$

where $J_i^{\rm old}$ is the mean intensity at the grid-point 'i' calculated via a formal solution of the RT equation using the current estimate of the source function (i.e. using $S_j^{\rm old}$ at all the grid-points j). For a given spatial grid of $\rm N_P$ points the formal solution of the transfer equation can be symbolically represented as

$$\mathbf{I}_{\vec{\Omega}} = \mathbf{\Lambda}_{\vec{\Omega}}\,[\mathbf{S}] + \mathbf{T}_{\vec{\Omega}}, \tag{4}$$

where $\mathbf{T}_{\vec{\Omega}}$ gives the transmitted specific intensity due to the incident radiation at the boundary and $\mathbf{\Lambda}_{\vec{\Omega}}$ is a $\rm N_P \times N_P$ operator whose elements depend on the optical distances between the grid-points. Thus, the mean intensity at the grid-point 'i' would be:

$$J_i = \Lambda_{i,1}S_1^a + ... + \Lambda_{i,i-1}S_{i-1}^a + \Lambda_{i,i}S_i^b + \Lambda_{i,i+1}S_{i+1}^c + ... + \Lambda_{i,\rm N_P}S_{\rm N_P}^c + T_i\,. \tag{5}$$

In this last expression $\Lambda_{i,j} = \sum(\Lambda_{i,j}^{in} + \Lambda_{i,j}^{out})/2$ (with the sum applied to all the directions $\vec{\Omega}$ of the numerical angular quadrature) and a, b and c are simply symbols that we use as a notational trick to indicate below whether we choose the 'old' or the 'new' values of the source function. Thus, for instance, the Λ-iteration method consists in calculating J_i choosing $a = b = c =$ old, which gives $J_i = J_i^{\rm old}$ as indicated in Eq. (3).

The Jacobi method, known in the RT literature as the local ALI method (see Olson, Auer and Buchler, 1986), and on which most Non-LTE codes are based on, is found by choosing $a = c =$ old, but $b =$ new, which yields

$$J_i = J_i^{\rm old} + \Lambda_{i,i}\,(S_i^{\rm new} - S_i^{\rm old}) = J_i^{\rm old} + \Lambda_{i,i}\,\delta S_i\,. \tag{6}$$

In fact, using this expression instead of $J_i^{\rm old}$ in Eq. (3) we find that the resulting Jacobi iterative scheme is

$$S_i^{\rm new} = S_i^{\rm old} + \delta S_i, \tag{7}$$

with the correction

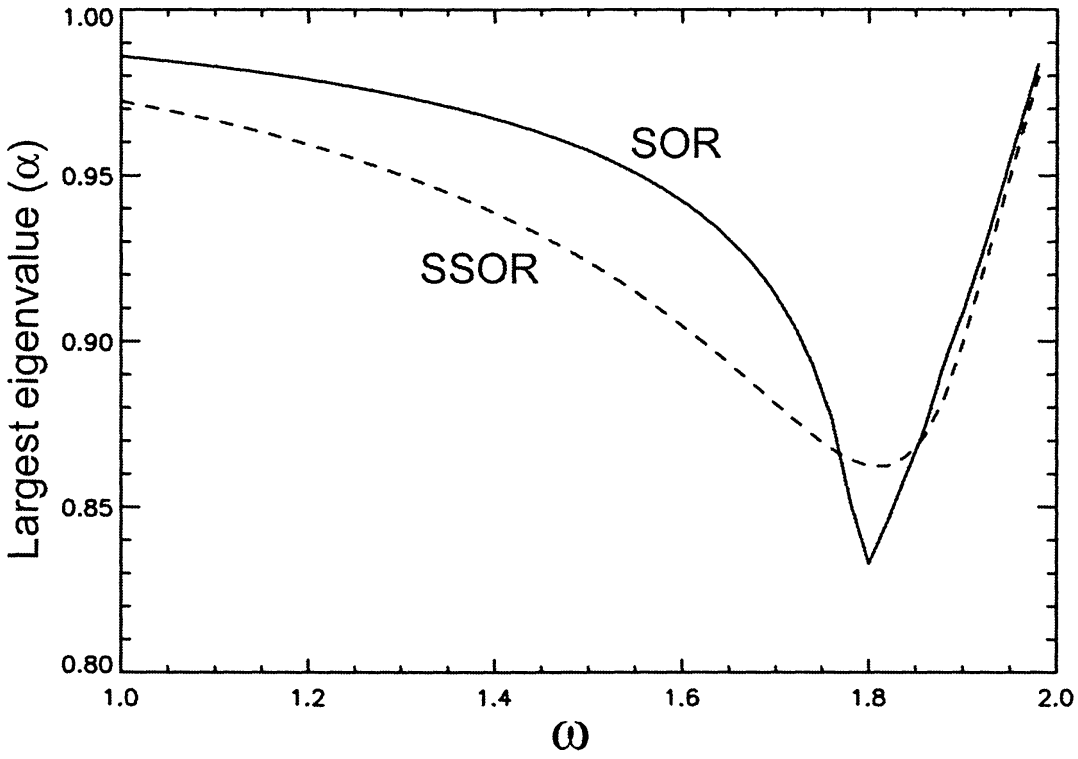

Figure 1. The sensitivity of the maximum absolute eigenvalue (α) of the iteration operators of the SOR and SSOR methods to the choice of the ω parameter. (These results have been obtained from Non-LTE calculations in an isothermal atmosphere of two-level atoms with $\epsilon = 10^{-4}$). The pure GS method that results when applying the SSOR strategy with $\omega = 1$ is four times faster than Jacobi (i.e. than the local ALI method), while SOR with the optimum ω value is 10 times faster. Fortunately, the rate of convergence of SSOR is relatively insensitive to the exact choice of ω so that a precise optimum value of ω is not crucial for achieving an extremely high convergence rate. The α-value for $\omega = 1$ gives the convergence rate of the pure GS method.

$$\delta S_i = \frac{[(1-\epsilon)J_i^{\rm old} + \epsilon B_i - S_i^{\rm old}]}{[1-(1-\epsilon)\Lambda_{i,i}]}, \tag{8}$$

where $\Lambda_{i,i}$ at the spatial grid-point 'i' is the corresponding *diagonal element* of the Λ-operator, which can be obtained easily while doing the formal solution of the RT equation for calculating $J_i^{\rm old}$ (e.g. via a formal solver based on the 'short-characteristics' method described by Kunasz & Auer 1988).

A superior type of RT methods are those developed by Trujillo Bueno & Fabiani Bendicho (1995; hereafter TF95), which are based on Gauss-Seidel (GS) iterations. This type of iterative schemes are obtained by choosing c = old and $a = b$ = new in Eq. (5). This yields

$$J_i = J_i^{\rm old+new} + \Lambda_{i,i}\,\delta S_i, \tag{9}$$

where $J_i^{\rm old+new}$ is the mean intensity calculated using the 'new' values of the source function at grid-points 1,2,...,$i-1$ and the 'old' values at points $i, i+1, ..., {\rm N_P}$. The iterative correction is given by

$$\delta S_i^{\rm GS} = \frac{[(1-\epsilon)J_i^{\rm old+new} + \epsilon B_i - S_i^{\rm old}]}{[1-(1-\epsilon)\Lambda_{i,i}]} . \qquad (10)$$

It is very important to clarify the meaning of this last equation:

1) First, at point $i = 1$ (which we can freely assign to any of the two boundaries of the medium under consideration) use 'old' source function values to calculate J_1 via a formal solution. Apply Eqs. (10) and (7) to calculate $S_1^{\rm new}$.

2) Go to the next point $i = 2$ and use $S_1^{\rm new}$ and the "old" source-function values $S_j^{\rm old}$ at points $j = 2, 3, ..., {\rm N_P}$ to get J_2 via a formal solution. Apply Eqs. (10) and (7) to calculate $S_2^{\rm new}$.

3) Go to the next spatial point k and use the previously obtained 'new' source function values at $j = 1, 2, ..., k-1$, but the still 'old' ones at $j = k, k+1, ..., {\rm N_P}$ to get J_k via a formal solution and $S_k^{\rm new}$ as dictated by Eqs. (10) and (7).

4) Go to the next point $k+1$ and repeat what has just been indicated in the previous point until arriving to the other boundary point.

The result of what we have just indicated is a pure GS iteration. A SOR iteration is obtained by doing the corrections as follows:

$$\delta S_i^{\rm SOR} = \omega\, \delta S_i^{\rm GS}, \qquad (11)$$

where ω is a parameter with an optimum value between 1 and 2 which can be found easily (see section 2.4 of TF95). Obviously, the optimum ω-value is that which leads to the highest rate of convergence, i.e. that which minimizes the *maximum absolute eigenvalue* (α) of the iteration operator of the iterative scheme. Note that α gives the *asymptotic rate of convergence* of the iterative method and that the number of iterations required to reduce the error by a given factor is inversely proportional to $-ln(\alpha)$ (see TF95). The solid line of Fig. 1 gives the sensitivity of the convergence rate of our SOR radiative transfer method to the parameter ω, showing that it is very significant. Although the selection criterion for the optimum ω-value proposed by TF95 is robust enough to guarantee the effectiveness of their SOR radiative transfer method, one would be much happier with a RT method characterized by a similar convergence rate, but having a considerably reduced sensitivity to the ω parameter (which lies always between 1 and 2).

Has such a RT method been developed? The answer is affirmative, as shown by the dashed line of Fig. 1. It is a Symmetric SOR (SSOR) method which has some very interesting mathematical properties (e.g. Hageman & Young 1981). The corresponding GS limit (i.e. the case with $\omega = 1$) goes exactly as indicated previously, but with the fourth step modified as follows:

4) Go to the next point $k+1$ and repeat what has just been indicated in the previous point until arriving to the other boundary point. Having reached this boundary point initiate again the same process, *but choosing now as first point $i = 1$ this boundary point.*

The basic idea of this RT method was clearly indicated in the conclusions of TF95. With respect to their original GS-based technique the improved GS-based method yields the converged solution with a factor 2 of saving in the total computational work, simply because the ensuing formal solver produces *two* (instead of just one!) GS iterations: one after the *incoming* pass with the formal solver and an extra one after the *outgoing* pass. The application of the same iterative scheme, but with $1 < \omega < 2$, produces the SSOR method (see the dashed line of Fig. 1). Note that its rate of convergence is relatively insensitive to the exact choice of ω so that a precise optimum value of ω is not crucial. An additional interesting feature is that, contrary to what happens with the original SOR technique of TF95, the SSOR method for RT applications can be combined with standard acceleration techniques (e.g. with Ng's acceleration) in order to achieve even faster convergence (Trujillo Bueno 2002)[4].

Finally, it is helpful to remember that all these methods are based on the idea of operator splitting. Therefore, they are characterized by a convergence rate which *decreases* as the resolution of the spatial grid is increased. As a result, if N_P is the number of grid-points in a computational box of *fixed* dimensions, the computing time or computational work (W) required by these iterative methods to yield the self-consistent atomic (or molecular) level populations scales with N_P as follows:

- Jacobi-based ALI method $\rightarrow$ $W \sim {N_P}^2$
- GS-based method $\rightarrow$ $W \sim {N_P}^2/4$
- SOR method $\rightarrow$ $W \sim N_P\sqrt{N_P}$

The only available multilevel RT method that yields $W \sim N_P$ is the *non-linear multigrid method*, which is of particular interest for 3D applications where $N_P \approx 10^6$ (see Fabiani Bendicho, Trujillo Bueno & Auer, 1997). In section 2.1 of the just quoted paper the interested reader can find a brief description of our "MUltilevel GAuss-Seidel" method (MUGA), which is the generalization of the GS-based method of TF95 to the non-linear multilevel case. MUGA is actually the method of choice for the smoothing part of the non-linear multigrid iteration.

4. The Zeeman effect, optical pumping and the Hanle effect

The Zeeman effect requires the presence of a magnetic field, which causes the atomic energy levels to split into different magnetic sublevels characterized by their magnetic quantum number M. This Zeeman splitting produces local *sources* and *sinks* of light polarization because of the ensuing wavelength shifts between the π ($\Delta M = M_u - M_l = 0$) and σ ($\Delta M = M_u - M_l = \pm 1$) transitions. The Zeeman effect is most sensitive in *circular* polarization, with a magnitude that for not too strong fields scales with the ratio between the Zeeman splitting and the width of the spectral line (which is very much larger than the natural width of the atomic levels) and in a way such that the Stokes $V(\lambda)$ profile

[4]As a result, the reader may prefer to call it "Super SOR".

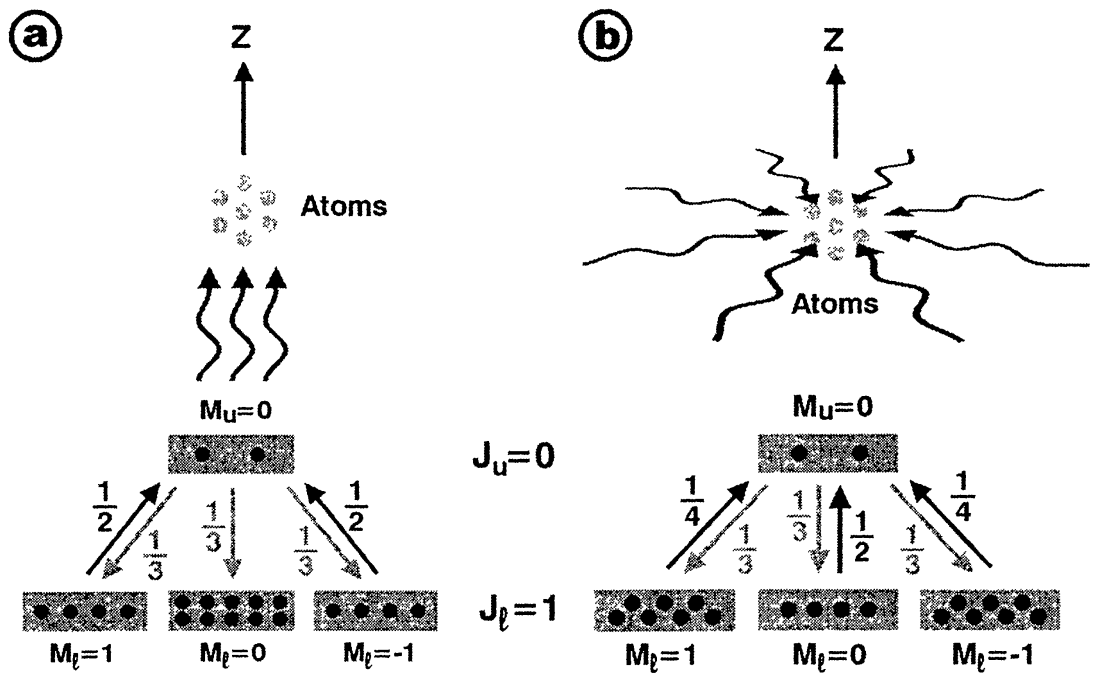

Figure 2. Illustration of the *atomic polarization* that is induced in the lower level of a two-level atom (with $J_l = 1$ and $J_u = 0$) by two types of anisotropic illuminations (**a** and **b**). The incident radiation field is assumed to be unpolarized and with axial symmetry around the vertical direction, which is our choice here for the quantization axis of total angular momentum. In both cases, an excess population tends to build up in the weakly absorbing sublevels. Note that the alignment coefficient of the lower level (i.e. $\rho^2_0 = (N_1 - 2N_0 + N_{-1})/\sqrt{6}$, being N_i the populations of the magnetic sublevels) is *negative* in case (**a**) (where the incident beam is *parallel* to the quantization axis), but *positive* in case (**b**) (where the incident beams are *perpendicular* to the quantization axis). The physical understanding of the information provided in this figure is left as an exercise to the reader.

changes its sign for opposite orientations of the magnetic field vector. This so-called *longitudinal* Zeeman effect responds to the line-of-sight component of the magnetic field. In contrast, the *transverse* Zeeman effect responds to the component of the magnetic field perpendicular to the line of sight, but produces *linear* polarization signals that are normally negligible for magnetic strengths B < 100 gauss.

In contrast, the spectral line polarization that is induced by scattering processes in the outer layers of stellar atmospheres is directly related with the anisotropic illumination of the atoms. Anisotropic radiation pumping produces *atomic level polarization*–that is, population imbalances and quantum interferences between the sublevels of degenerate atomic levels. Such a pumping is *selective* (e.g. Kastler 1950). For example, **upper-level population pumping** occurs when some *upper state* sublevels have more chance of being populated

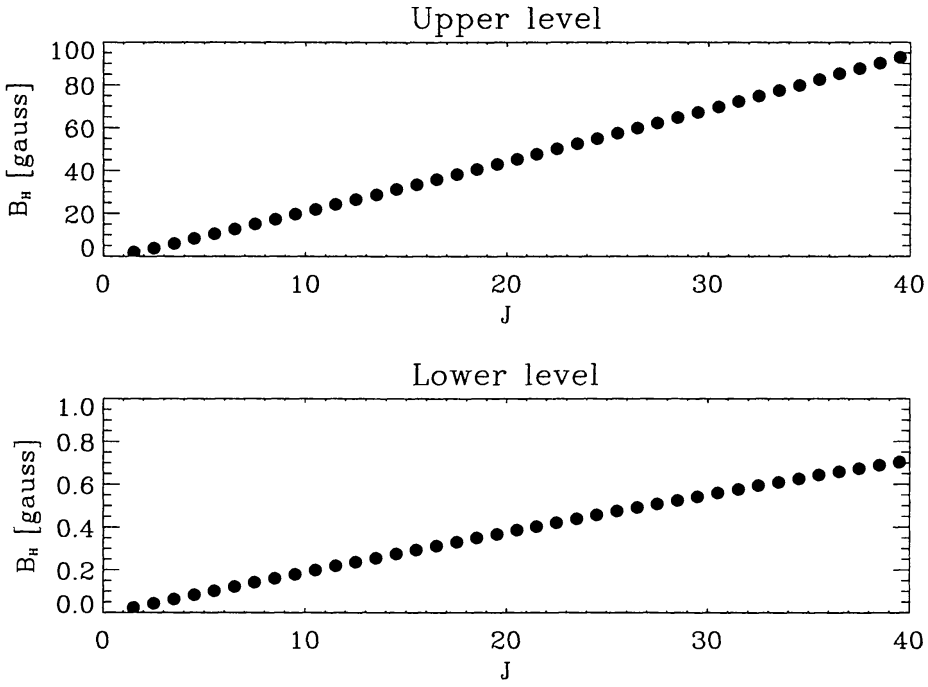

Figure 3. Example of the application of the basic formula of the Hanle effect to the lower and upper levels of MgH lines that produce scattering polarization on the Sun. Each point refers to a spectral line of the Q branch, whose lines have $J_l = J_u = J$.

than others. On the contrary, as illustrated in Fig. 2, **lower-level depopulation pumping** occurs when some *lower state* sublevels absorb light more strongly than others. As a result, an excess population tends to build up in the weakly absorbing sublevels. It is also important to note that line transitions between levels having other total angular momentum values (e.g., $J_l = J_u = 1$) permit the transfer of atomic polarization between both levels via a process called **repopulation pumping** (e.g. lower-level atomic polarization can result simply from the spontaneous decay of a *polarized* upper level).

The presence of a magnetic field is *not* necessary for the operation of such optical pumping processes, which can be particularly efficient in creating atomic polarization if the depolarizing rates from elastic collisions are sufficiently low. The Hanle effect is the modification of the atomic-level polarization (and of its ensuing observable effects on the emergent Stokes Q and U profiles) caused by the action of a magnetic field such that its corresponding Zeeman splitting is comparable to the inverse lifetime of the degenerate atomic level under consideration (Hanle 1924; see the review by Trujillo Bueno 2001). For the Hanle effect to operate, the magnetic field vector ($\mathbf{B}$) has to be significantly *inclined* with respect to the symmetry axis of the pumping radiation field.

A useful formula to estimate the magnetic field intensity $B_{\rm H}$ (measured in gauss) to which the Hanle effect can (in principle) be sensitive is

$$2\pi\nu_L\, g_J \;=\; 8.79{\times}10^6\; B_{\rm H}\; g_J \;\approx\; 1/t_{\rm life}\;, \tag{12}$$

where ν_L is the Larmor frequency, while g_J and $t_{\rm life}$ are, respectively, the Landé factor and the lifetime (in seconds) of the atomic level under consideration (which can be either the upper or the lower level of the chosen spectral line). This formula shows that the measurement and physical interpretation of weak polarization signals in suitably chosen spectral lines may allow us to diagnose magnetic fields having intensities between 10^{-3} and 100 gauss approximately, *i.e.*, in a parameter domain that is very hard to study via the Zeeman effect alone. Fig. 3 shows an illustrative example of the type of information that this formula may provide.

In general, the physical interpretation of polarization signatures in spectral lines requires to find the diagonal and non-diagonal elements of the atomic density matrix (associated to each level of total angular momentum J of the chosen atomic or molecular system) which are *consistent* with both the *intensity* and *polarization* of the radiation field generated within the (generally magnetized) stellar atmospheric model under consideration. This is a very involved *non-local* and *non-linear* RT problem for which the term **'Non-LTE of the Second Kind'** has been proposed (Landi Degl'Innocenti 2002). The numerical solution of this Non-LTE problem, which lies at the basis of 'Astrophysical Spectropolarimetry', is addressed below after a brief review of the basic equations.

5. The rate equations for the elements of the atomic density matrix

As illustrated in Fig. 2, the concept of overall population of each level of total angular momentum J is not sufficient to describe the excitation state of a *polarized* atomic or molecular system. In general, one has to use the mixed state density operator ($\rho^{\rm A}$) of quantum mechanics (e.g. Fano 1957). This operator is represented in the basis of eigenvectors of the total angular momentum via a matrix called the atomic density matrix whose $(2J+1)^2$ elements are:

$$\rho^{\rm A}_{\alpha J}(M,M') \;=\; \langle \alpha JM|\rho^{\rm A}|\alpha JM'\rangle, \tag{13}$$

where $\rho^{\rm A}_{\alpha J}(M,M)$ is the population of the sublevel with magnetic quantum number M, while $\rho^{\rm A}_{\alpha J}(M,M')$ (with $M{\neq}M'$) quantifies the degree of quantum interference (or coherence) between the magnetic sublevels M and M' pertaining to the level of total angular momentum J.

In the context of scattering polarization and the Hanle effect it is more convenient to quantify the atomic polarization of a given level by means of the following linear combinations of the $\rho^{\rm A}_{\alpha J}(M,M')$ elements (e.g. Omont 1977):

$$\rho^K_Q(\alpha J) = \sum_{MM'} (-1)^{J-M}\sqrt{2K+1}\begin{pmatrix} J & J & K \\ M & -M' & -Q \end{pmatrix}\rho^{\rm A}_{\alpha J}(M,M'), \tag{14}$$

where the 3-j symbol is defined as indicated by any suitable textbook on Racah algebra (e.g. Brink & Satchler 1968). It is important to note that $0{\leq}K{\leq}2J$ and $-K{\leq}Q{\leq}K$. The ρ^K_Q elements with $Q=0$ are *real* numbers given by linear combinations of the populations of the various Zeeman sublevels corresponding to

the level of total angular momentum J. The total population of the atomic level is quantified by $\sqrt{2J+1}\rho^0_0$, while the population imbalances among the Zeeman sublevels are quantified by ρ^K_0 (e.g. $\rho^2_0(J=1) = (N_1 - 2N_0 + N_{-1})/\sqrt{6}$). However, the ρ^K_Q elements with $Q \neq 0$ are *complex* numbers given by linear combinations of the *coherences* between Zeeman sublevels whose magnetic quantum numbers differ by Q. In fact, since the density operator is Hermitian, we have that for each spherical statistical tensor component ρ^K_Q with $Q > 0$, there exists another component with $Q < 0$ given by $\rho^K_{-Q} = (-1)^Q[\rho^K_Q]^*$. We thus have $(2J+1)^2$ density-matrix elements corresponding to each level of total angular momentum J. The ρ^0_0 elements produce the dominant contribution to the Stokes I parameter. The ρ^2_Q elements (the *alignment* components) contribute to the *linear* polarization signals, which we quantify by the Stokes parameters Q and U (see sections 8.1, 8.2, 9.1 and 9.2). The ρ^1_Q elements (the *orientation* components) contribute to the circular polarization (see the second point of section 8.3).

For the case of a multilevel atom devoid of hyperfine structure and taking into account quantum coherences only between the sublevels pertaining to each J-level, the rate of change of the density matrix element $\rho^K_Q(J)$ *in the magnetic field reference system* reads[5] (Landi Degl'Innocenti 1983, 1985):

$$\frac{d}{dt}\rho^K_Q(J) = -2\pi i \nu_L\, g_J\, Q\, \rho^K_Q(J) \tag{15}$$

$$+ \sum_{J_l} \sum_{K_l Q_l} \rho^{K_l}_{Q_l}(J_l)\, T_{\rm A}(J_l; K_l\, Q_l \rightarrow J; K\, Q)$$

$$+ \sum_{J_u} \sum_{K_u Q_u} \rho^{K_u}_{Q_u}(J_u)\, T_{\rm E}(J_u; K_u\, Q_u \rightarrow J; K\, Q)$$

$$+ \sum_{J_u} \sum_{K_u Q_u} \rho^{K_u}_{Q_u}(J_u)\, T_{\rm S}(J_u; K_u\, Q_u \rightarrow J; K\, Q)$$

$$- \sum_{K' Q'} \rho^{K'}_{Q'}(J)\, R_{\rm A}(J; K\, Q, K'\, Q' \rightarrow J_u)$$

$$- \sum_{K' Q'} \rho^{K'}_{Q'}(J)\, R_{\rm E}(J; K\, Q, K'\, Q' \rightarrow J_l)$$

$$- \sum_{K' Q'} \rho^{K'}_{Q'}(J)\, R_{\rm S}(J; K\, Q, K'\, Q' \rightarrow J_l)$$

$$- D^{(K)}(J)\, \rho^K_Q(J),$$

where $\nu_L = 1.39 \times 10^6\, B$ is the Larmor frequency (with the magnetic field strength B in gauss). Eqs. (15) indicate that *in the magnetic field reference*

[5]This is the reference system with the quantization axis of total angular momentum parallel to the magnetic field vector.

system the population imbalances (i.e. the ρ^K_Q density-matrix elements with $Q = 0$) are *insensitive* to the magnetic field, while the coherences (i.e. the ρ^K_Q elements with $Q \neq 0$) are *reduced* and *dephased* as the magnetic field strength increases. We note that the limiting case in which polarization phenomena are neglected (cf. Mihalas 1978) is obtained by retaining only the terms with $K = Q = 0$ and neglecting the Zeeman splittings.

The last term of Eq. (15) is the contribution of *elastic* collisions to the rate of change of $\rho^K_Q(J)$, since $D^{(K)}$ is the *depolarizing* collisional rate for the density-matrix element of rank K (e.g. Lamb & Ter Haar 1971). For notational simplicity, Eq. (15) does not include the contribution of *inelastic* collisional rates. However, the scattering polarization calculations shown below do take them fully into account. It is more interesting to focus on the radiative rates, both on the *transfer* rates due to absorption (T_A), spontaneous emission (T_E) and stimulated emission (T_S) *from* other levels, and on the *relaxation* rates due to absorption (R_A), spontaneous emission (R_E) and stimulated emission (R_S) *towards* other levels. The explicit expressions for all these transfer and relaxation rates can be found in Bommier & Sahal-Bréchot (1978) and Landi Degl'Innocenti (1983, 1984, 1985). Of particular interest are the transfer rate $T_{\rm A}$ due to *absorption* from lower levels and the transfer rate $T_{\rm E}$ due to *spontaneous emissions* from upper levels.

Let us first consider the expression for T_A (Landi Degl'Innocenti 1983):

$$T_{\rm A}(J_l;K_lQ_l \rightarrow J;KQ) = (2J_l{+}1)B(J_l \rightarrow J) \sum_{K_{\rm r}Q_{\rm r}} \sqrt{3(2K+1)(2K_l+1)(2K_{\rm r}+1)} \times (-1)^{K_l+Q_l} \left\{ \begin{array}{ccc} J & J_l & 1 \\ J & J_l & 1 \\ K & K_l & K_{\rm r} \end{array} \right\} \left(\begin{array}{ccc} K & K_l & K_{\rm r} \\ -Q & Q_l & -Q_{\rm r} \end{array} \right) \bar{J}^{K_{\rm r}}_{Q_{\rm r}}, \quad (16)$$

where $\bar{J}^{K_{\rm r}}_{Q_{\rm r}}$, with $K_{\rm r} = 0, 1, 2$, and $Q_{\rm r} = -K_{\rm r}, ..., K_{\rm r}$, are radiation field tensors given by integrals over frequency and solid angle of the Stokes parameters, weighted by suitable frequency and angular functions (see their explicit expressions in section 3 of Trujillo Bueno 2001). We point out that $\bar{J}^0_0$ is the familar $\bar{J}$-quantity of the standard Non-LTE problem (which is an average over frequencies and directions of the Stokes I parameter weighted by the absorption profile), while

$$\bar{J}^2_0 = \int {\rm d}x \oint \phi_x \frac{{\rm d}\vec{\Omega}}{4\pi} \frac{1}{2\sqrt{2}} \left[(3\mu^2 - 1) I_{x\vec{\Omega}} + 3(\mu^2 - 1) Q_{x\vec{\Omega}} \right], \quad (17)$$

where ϕ_x is the absorption line shape and x the frequency distance from line center measured in units of the Doppler width. This $\bar{J}^2_0$ tensor, which is dominated by the contribution of the Stokes I parameter, provides information on the 'degree of anisotropy' of the radiation field. For instance, let us assume a one-dimensional plane-parallel atmosphere with the Z-axis along the vertical. In the absence or in the presence of a microturbulent and isotropic magnetic field, the only non-zero radiation field tensors are $\bar{J}^0_0$ and $\bar{J}^2_0$. Therefore, a funda-

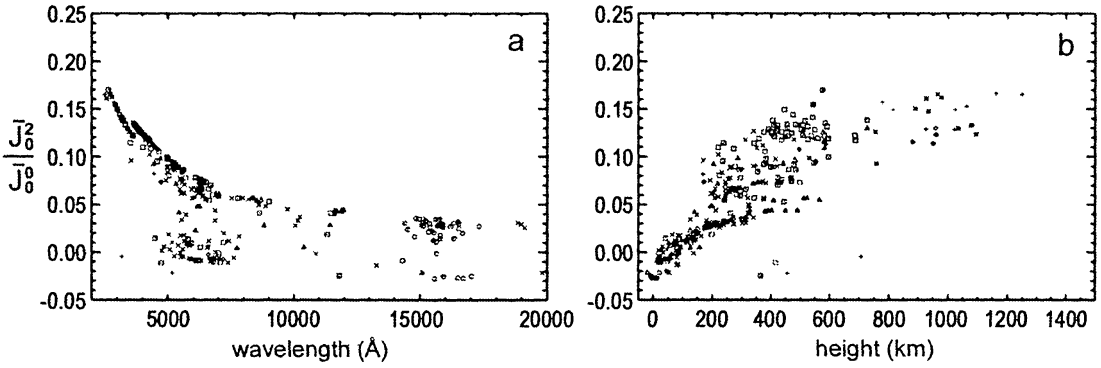

Figure 4. The 'anisotropy factor' in solar Fe I lines. For each iron line of a realistic multilevel model (see Shchukina & Trujillo Bueno 2001) the figures show the value of $\mathcal{A}$ at the atmospheric height where $\tau_{\rm line} = 1$ along the line of sight for a simulated observation at $\mu = 0.1$.

mental quantity in scattering polarization is the 'anisotropy factor' $\mathcal{A} = \bar{J}^2_0/\bar{J}^0_0$, whose possible values are bounded as dictated by the following expression[6]:

$$-\frac{1}{2} \leq \sqrt{2}\mathcal{A} \leq 1. \tag{18}$$

In the chosen reference system (with the Z-axis along the vertical), the largest value corresponds to an illumination coming from a purely vertical radiation beam (case (**a**) of Fig. 2) and the lowest one to a purely horizontal radiation field without any azimuthal dependence (case (**b**) of Fig. 2). Figure 4 of Trujillo Bueno (2001) gives the variation of $\mathcal{A}$ with line optical depth in Milne-Eddington atmospheres, showing that $\mathcal{A}$ increases with the source function gradient. An additional interesting example is given in Fig. 4, which shows the $\mathcal{A}$ values for many lines of the Fe I spectrum resulting from a self-consistent Non-LTE calculation in a semi-empirical model of the solar atmosphere.

We now turn our attention to the transfer rate due to spontaneous emissions from upper levels (Landi Degl'Innocenti 1983):

$$T_{\rm E}(J_u; K_u\, Q_u \rightarrow J; K\, Q) = \delta_{KK_u}\delta_{QQ_u}\,(-1)^{1+J+J_u+K} \left\{ \begin{array}{ccc} J_u & J_u & K \\ J & J & 1 \end{array} \right\}$$

$$\times\, (2J_u + 1) A(J_u \rightarrow J) \tag{19}$$

This expression and the corresponding term of Eq. (15) clearly indicate that the atomic polarization of a given level can simply result from the spontaneous decay of a *polarized* upper level. As mentioned in section 4, this is known as *repopulation pumping.*

[6]Note that there is a typing error in Eq. (11) of Trujillo Bueno (2001), since the inequality given there is correct for $2\mathcal{A}$ and *not* for $\mathcal{A}$, as it was typed.

6. Formal solvers of the Stokes-vector transfer equation

In the polarized case, instead of the standard RT equation for the specific intensity $I(x,\vec{\Omega})$ one has to solve, in general, the following *vectorial* transfer equation for the Stokes vector $\mathbf{I}(x,\vec{\Omega}) = (I,Q,U,V)^\dagger$ (with $\dagger$=transpose)

$$\frac{d}{ds}\begin{pmatrix} I \\ Q \\ U \\ V \end{pmatrix} = \begin{pmatrix} \epsilon_I \\ \epsilon_Q \\ \epsilon_U \\ \epsilon_V \end{pmatrix} - \begin{pmatrix} \eta_I & \eta_Q & \eta_U & \eta_V \\ \eta_Q & \eta_I & \rho_V & -\rho_U \\ \eta_U & -\rho_V & \eta_I & \rho_Q \\ \eta_V & \rho_U & -\rho_Q & \eta_I \end{pmatrix} \begin{pmatrix} I \\ Q \\ U \\ V \end{pmatrix}. \qquad (20)$$

This equation, whose QED derivation can be found in Landi Degl'Innocenti (1983), can be written in more compact notation as follows:

$$\frac{d}{ds}\mathbf{I} = \mathbf{e} - \mathbf{K}\mathbf{I}, \qquad (21)$$

where s measures the geometrical distance along the ray of direction $\vec{\Omega}$, $\mathbf{K}$ is the absorption (or propagation) matrix and $\mathbf{e}$ is the emission vector. Alternatively, introducing the optical depth $\mathrm{d}\tau = -\eta_I \mathrm{d}s$,

$$\frac{d}{d\tau}\mathbf{I} = \mathbf{K}^*\mathbf{I} - \mathbf{S}, \qquad (22)$$

where $\mathbf{K}^* = \mathbf{K}/\eta_I$ and $\mathbf{S} = \mathbf{e}/\eta_I$.

Let us consider three spatial points (points M, O and P) situated along the direction $\vec{\Omega}$ of a ray propagating in a given spatial grid. Point O is the *grid-point* of interest at which one wishes to calculate the Stokes vector $\mathbf{I}_\mathrm{O}$ for a given frequency (x) and direction ($\vec{\Omega}$). Point M is the intersection point with the grid-plane that one finds when moving along $-\vec{\Omega}$. At this *upwind* point the Stokes vector $\mathbf{I}_\mathrm{M}$ (for the same frequency and angle) is known from previous steps. In a similar way, point P is the intersection point with the grid-plane that one encounters when moving along $\vec{\Omega}$. We also introduce the optical depths along the ray between points M and O ($\Delta\tau_\mathrm{M}$) and between points O and P ($\Delta\tau_\mathrm{P}$). ¿From the formal solution of Eq. (22) one finds that the Stokes-vector at the grid-point O is

$$\mathbf{I}_\mathrm{O} = \mathbf{O}(0,\Delta\tau_\mathrm{M})\mathbf{I}_\mathrm{M} + \int_0^{\Delta\tau_\mathrm{M}} \mathbf{O}(t,\Delta\tau_\mathrm{M})\,\mathbf{S}(t)\,dt, \qquad (23)$$

where $\mathbf{O}(t,\Delta\tau_\mathrm{M})$ is the evolution operator (i.e. the 4×4 Mueller matrix of the atmospheric slab between t and $\Delta\tau_\mathrm{M}$). In general, this evolution operator does not have an easy analytical expression (see Landi Degl'Innocenti & Landi Degl'Innocenti, 1985) and, therefore, the integral of the previous equation cannot be solved analytically. However, if the 4×4 absorption matrix $\mathbf{K}^*$ conmutes between depth points M and O (e.g. because one assumes that matrix $\mathbf{K}^*$ is constant between M and O and equal to its true value at the middle point) the evolution operator reduces then to an expression given by the exponential of the absorption matrix. The integral of Eq. (23) can then be solved analytically assuming that the source function vector $\mathbf{S}$ varies parabolically along M, O and

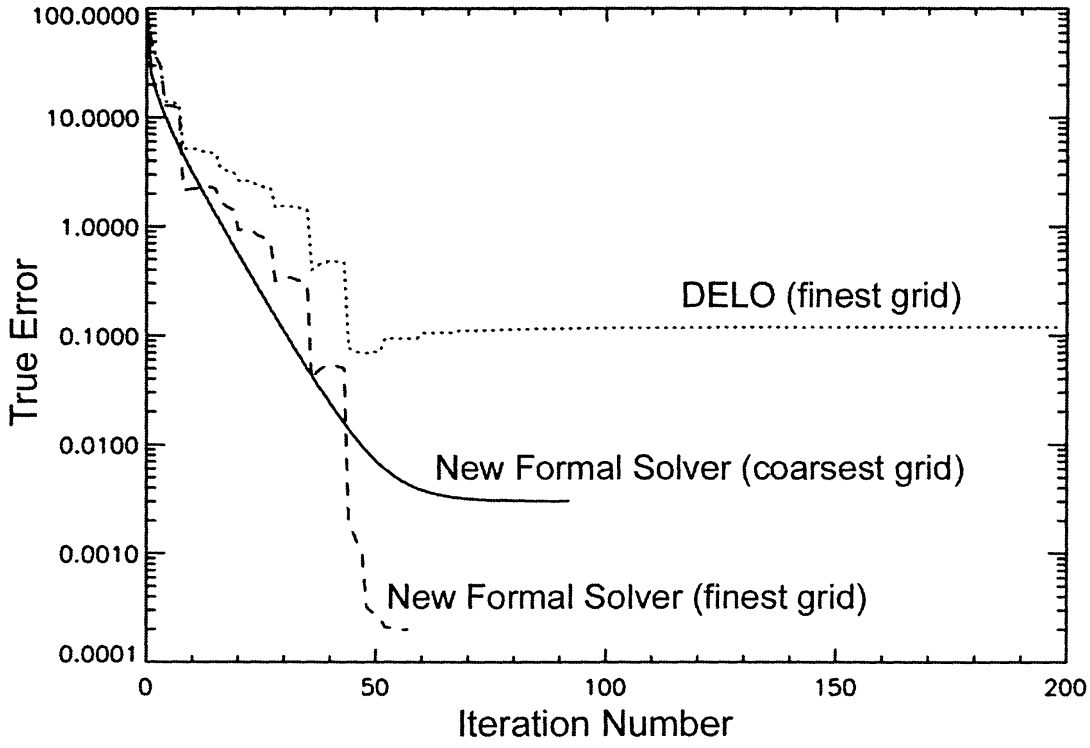

Figure 5. The variation of the maximum relative *true error* versus the iteration number for three Non-LTE Zeeman line transfer calculations (see section 8.3). Dotted line corresponds to the local ALI method with Ng acceleration in combination with the original DELO formal solver using $n = 20$ spatial grid-points per decade (the finest grid). The dashed line corresponds to Jacobi with Ng acceleration, but using our formal solution solver with $n = 20$ points per decade. The solid line corresponds to an iterative calculation without Ng acceleration for a grid with $n = 9$ (the coarsest grid) and using our formal solution method of the Stokes-vector transfer equation.

P. The first of the two formal solution methods presented here is precisely based on this idea and the result is

$$\mathbf{I}_{\mathrm{O}} = \mathbf{O}(0, \Delta\tau_{\mathrm{M}})\mathbf{I}_{\mathrm{M}} + \mathbf{\Psi}_{\mathrm{M}}\mathbf{S}_{\mathrm{M}} + \mathbf{\Psi}_{\mathrm{O}}\mathbf{S}_{\mathrm{O}} + \mathbf{\Psi}_{\mathrm{P}}\mathbf{S}_{\mathrm{P}}, \tag{24}$$

where $\mathbf{\Psi}_{\mathrm{X}}$ (with X either M, O or P) are 4×4 matrices which are given in terms of $\Delta\tau_{\mathrm{M}}$ and $\Delta\tau_{\mathrm{P}}$, in terms of the inverse of the absorption matrix $\mathbf{K}^*$ and in terms of the analytical expression given by Landi Degl'Innocenti & Landi Degl'Innocenti (1985) for the evolution operator.

Figure 5 shows a comparison between two different calculations performed with the iterative methods we have developed for solving the Non-LTE Zeeman line transfer problem outlined in section 8.3. One of such calculations was carried out combining ALI with the DELO formal solution method of Rees, Murphy & Durrant (1989), while the second Non-LTE calculation was performed using the new formal solution method. The figure gives the variation of the maximum

relative *true error* (T_e) versus the iteration number. It demonstrates that DELO is not sufficiently accurate for self-consistent Non-LTE calculations. Note that, even with $n = 20$ spatial grid-points per decade, the Non-LTE calculation using DELO as formal solver gives a maximum *true error* of the order of 10%. However, our formal solution solver for polarization transfer assumes that the source function vector varies parabolically and this is indeed suitable for Non-LTE calculations yielding a $T_e < 1\%$ already for $n = 9$. This new formal solution method can be considered as a generalization, to the polarization case, of the short-characteristics method of Kunasz & Auer (1988), which is often applied for solving 1D, 2D and 3D Non-LTE unpolarized transfer problems. The Non-LTE Zeeman line transfer calculations of Trujillo Bueno & Landi Degl'Innocenti (1996) were performed combining this Stokes-vector formal solver with the iterative schemes discussed in section 8.3.

The reason why the DELO method, as originally formulated, is not suitable for Non-LTE polarization transfer is because it is based on a *linear interpolation* approximation. However, it can be easily improved so as to make it a truly accurate formal solution method without deteriorating its efficiency. The original DELO method is based on the following transfer equation which can be easily derived from Eq. (22):

$$\frac{d}{d\tau}\mathbf{I} = \mathbf{I} - \mathbf{S}_{\rm eff}, \tag{25}$$

where the effective source-function vector $\mathbf{S}_{\rm eff} = \mathbf{S} - \mathbf{K}'\mathbf{I}$, being $\mathbf{K}' = \mathbf{K}^* - \mathbf{1}$ (with $\mathbf{1}$ the unit matrix). Therefore, the Stokes vector at grid-point O reads:

$$\mathbf{I}_{\rm O} = {\rm e}^{-\Delta\tau_M}\,\mathbf{I}_M + \int_0^{\Delta\tau_M} {\rm e}^{-(\Delta\tau_M - t)}\mathbf{S}_{\rm eff}(t)\,dt\,. \tag{26}$$

Assuming that $\mathbf{S}$ varies *parabolically* along M, O and P, but that $\mathbf{K}'\mathbf{I}$ varies *linearly* along M and O, we obtain:

$$[\mathbf{1} + \Psi'_O\,\mathbf{K}'_O]\mathbf{I}_O = [{\rm e}^{-\Delta\tau_{\rm M}}\,\mathbf{1} - \Psi'_M\,\mathbf{K}'_M]\,\mathbf{I}_M + \Psi_M\,\mathbf{S}_M + \Psi_O\,\mathbf{S}_O + \Psi_P\,\mathbf{S}_P\,, \tag{27}$$

where the $\Psi_{\rm X}$ functions (with X either M, O or P) are given in terms of the quantities $\Delta\tau_{\rm M}$ and $\Delta\tau_{\rm P}$, while $\Psi'_{\rm X}$ in terms of $\Delta\tau_{\rm M}$.

The big advantage of this improved DELO method (which I like to call 'DELOPAR') is that it is substantially more accurate than the original DELO method. Note that for the limiting case of negligible polarization DELOPAR has full parabolic accuracy, while DELO simply has linear accuracy. It is in fact a very suitable formal solver for obtaining the self-consistent solution of complicated Non-LTE polarization transfer problems, both for the Zeeman line transfer case (Trujillo Bueno & Landi Degl'Innocenti 1996) and for the solution of the multilevel Hanle effect problem (see Section 9.2). We have also applied it for developing a Non-LTE inversion code of Stokes profiles induced by the Zeeman effect (Socas-Navarro, Trujillo Bueno & Ruiz Cobo 2000a,b). Fabiani Bendicho & Trujillo Bueno (1999) indicate how these formal solution methods of the Stokes-vector transfer equation can be generalized to the 3D case with horizontal periodic boundary conditions.

7. Emission and absorption coefficients

The general expressions of the components of the emission vector and of the absorption matrix are very involved and will not be written here (see Landi Degl'Innocenti 1983). They are given in terms of the ρ^K_Q elements of the upper and lower levels of the line transition under consideration and on line-shape profiles whose dependence on the magnetic quantum numbers cannot be neglected when the Zeeman splittings are a significant fraction of the spectral line width. Such general expressions simplify considerably for several cases of practical interest. Probably, the most familiar case is that of Zeeman line transfer *without* atomic level polarization, in which the polarization signatures are purely due to the wavelength shifts of the π and σ transitions between the magnetic sublevels of the upper and lower levels (e.g. Landi Degl'Innocenti 1992; Stenflo 1994). For the case of scattering line polarization in weakly magnetized regions of stellar atmospheres, the general expressions for the I, Q and U components of the emission vector reduce to

$$\epsilon_I = \epsilon_0\,\rho^0_0 + \epsilon_0 w^{(2)}_{J_u J_l}\Big\{\frac{1}{2\sqrt{2}}(3\mu^2-1)\rho^2_0 - \sqrt{3}\mu\sqrt{1-\mu^2}(\cos\chi\mathrm{Re}[\rho^2_1] - \sin\chi\mathrm{Im}[\rho^2_1]) + \frac{\sqrt{3}}{2}(1-\mu^2)(\cos 2\chi\,\mathrm{Re}[\rho^2_2] - \sin 2\chi\,\mathrm{Im}[\rho^2_2])\Big\}, \quad (28)$$

$$\epsilon_Q = \epsilon_0\, w^{(2)}_{J_u J_l}\Big\{\frac{3}{2\sqrt{2}}(\mu^2-1)\rho^2_0 - \sqrt{3}\mu\sqrt{1-\mu^2}(\cos\chi\mathrm{Re}[\rho^2_1] - \sin\chi\mathrm{Im}[\rho^2_1]) - \frac{\sqrt{3}}{2}(1+\mu^2)(\cos 2\chi\,\mathrm{Re}[\rho^2_2] - \sin 2\chi\,\mathrm{Im}[\rho^2_2])\Big\}, \quad (29)$$

$$\epsilon_U = \epsilon_0\, w^{(2)}_{J_u J_l}\sqrt{3}\Big\{\sqrt{1-\mu^2}(\sin\chi\mathrm{Re}[\rho^2_1] + \cos\chi\mathrm{Im}[\rho^2_1]) + \mu(\sin 2\chi\,\mathrm{Re}[\rho^2_2] + \cos 2\chi\,\mathrm{Im}[\rho^2_2])\Big\}, \quad (30)$$

where the ρ^K_Q values are those of the *upper* level of the line transition under consideration, $\epsilon_0 = (h\nu/4\pi)A_{ul}\phi_x\mathcal{N}\sqrt{2J_u+1}$ (with $\mathcal{N}$ the total number of atoms per unit volume), $w^{(2)}_{J_u J_l}$ is the quantity introduced by Landi Degl'Innocenti (1984) (which depends only on J_u and J_l), and where the orientation of the ray is specified by $\mu = \cos\theta$ (with θ the polar angle) and by the azimuthal angle χ. The elements η_I, η_Q and η_U of the absorption matrix are given by identical expressions (i.e. by $\eta_I = \epsilon_I$, $\eta_Q = \epsilon_Q$ and $\eta_U = \epsilon_U$), but with $\eta_0 = (h\nu/4\pi)B_{lu}\phi_x\mathcal{N}\sqrt{2J_l+1}$ instead of ϵ_0, $w^{(2)}_{J_l J_u}$ instead of $w^{(2)}_{J_u J_l}$ and with the ρ^K_Q values of the *lower* level of the line transition instead of those of the upper level (for the case in which stimulated emissions are neglected). Note that ϵ_Q and η_Q depend on both the population imbalances (ρ^2_0) and on the coherences (ρ^2_Q, with $Q = 1, 2$), while ϵ_U and η_U depend *only* on the quantum coherences[7].

[7] In these expressions, the reference direction for $Q > 0$ lies in the plane formed by the propagation direction and the Z-axis.

8. Linear Problems: the two-level atom without ground-level polarization

The following sub-sections summarize how the iterative schemes of section 3 can be generalized to several polarization transfer problems for which the operator **A** of Eq. (1) does not depend on the unknown **x**. To have this simplification, one needs to choose a two-level atomic model neglecting stimulated emissions and ground-level polarization[8].

8.1. Resonance line polarization and the Hanle effect of a microturbulent magnetic field

Let us consider first the polarization transfer problem that offers the easiest conceptual transition between unpolarized and polarized Non-LTE radiative transfer. We assume a two-level model atom neglecting atomic polarization in the lower level and a one-dimensional (1D) plane-parallel atmosphere taking into account the Hanle effect caused by the presence of a weak *microturbulent* and *isotropic* magnetic field. Since for this model atmosphere the radiation field has rotational symmetry with respect to the vertical to the stellar surface, the only non-vanishing Stokes parameters are I and Q[9]. As shown in detail by Trujillo Bueno & Manso Sainz (1999), the application of the general equations (15) to this two-level atom problem leads to the following SE equations:

$$S_0^0 = (1-\epsilon)\bar{J}_0^0 + \epsilon B_\nu, \tag{31}$$

$$S_0^2 = \mathcal{H}\frac{(1-\epsilon)}{1+\delta\,(1-\epsilon)}\, w^{(2)}_{J_u J_l}\bar{J}_0^2, \tag{32}$$

where (for $K=0$ and $K=2$)

$$S_0^K = \frac{2h\nu^3}{c^2}\frac{2J_l+1}{\sqrt{2J_u+1}}\rho_0^K(u)\,. \tag{33}$$

In Eq. (32) $\mathcal{H}$ is a Hanle depolarization factor which varies between 1 (for $\nu_{\rm L}/A_{ul}=0$, with $\nu_{\rm L}$ the Larmor frequency) and 0.2 (for $\nu_{\rm L}/A_{ul}\to\infty$), ϵ is the collisional destruction probability due to *inelastic* collisions, $\delta = D^{(2)}/A_{ul}$ is the collisional depolarizing rate due to *elastic* collisions measured in units of the Einstein A_{ul} coefficient, $\bar{J}_0^0$ and $\bar{J}_0^2$ are the only radiation field tensors that play a role in this particular scattering polarization problem, and ρ_0^0 and ρ_0^2 are the density-matrix elements of the upper level normalized to the overall population of the ground level. These two density matrix elements are here the only *unknowns* whose self-consistent values need be calculated at each spatial grid-point.

---

[8] In addition, one has to prescribe the line opacity, which is proportional to the overall population of the lower level.

[9] We are choosing the reference direction for $Q>0$ in the plane formed by the propagation direction and the vertical.

Since the ground level is assumed to be unpolarized and the chosen magnetic field is microturbulent with mixed polarities, the absorption matrix $\mathbf{K}$ of Eq. (21) is diagonal (i.e. $\mathbf{K} = \eta_I \mathbf{1}$, with $\mathbf{1}$ the 4×4 unit matrix). Therefore, the general Stokes-vector transfer equation (21) reduces to the following *uncoupled* equations[10]

$$\frac{\mathrm{d}}{\mathrm{d}\tau_x} I = I - S_I, \tag{34}$$

$$\frac{\mathrm{d}}{\mathrm{d}\tau_x} Q = Q - S_Q, \tag{35}$$

where τ_x is the monochromatic optical depth along the ray, while S_I and S_Q are the source function components of the Stokes parameters I and Q, respectively. The line contribution to S_I and S_Q depend on the values of S_0^0 and S_0^2:

$$S_I^{line} = S_0^0 + \frac{w^{(2)}_{J_u J_l}}{2\sqrt{2}} (3\mu^2 - 1) S_0^2, \tag{36}$$

$$S_Q^{line} = \frac{3 w^{(2)}_{J_u J_l}}{2\sqrt{2}} (\mu^2 - 1) S_0^2, \tag{37}$$

where $w^{(2)}_{J_u J_l}$ is the quantity introduced by Landi Degl'Innocenti (1984), which only depends on the values of J_u and J_l (e.g. $w^{(2)}_{1,0} = 1$, but $w^{(2)}_{0,1} = 0$). We thus see in Eq. (37) that the 'sources' of Stokes Q are the upper-level population imbalances (S_0^2), which in turn are created by *anisotropic* radiation pumping (see Eq. 32).

We now turn our attention to describing how the iterative methods of section 3 can be applied to solve this polarization transfer problem. As shown in detail by Trujillo Bueno & Manso Sainz (1999), it suffices with introducing into Eqs. (31) and (32) the following expressions:

$$\bar{J}_0^0(i) \approx \bar{J}_0^{0*}(i) + \Lambda_0^0(i,i)\, \delta S_0^0(i) + \Lambda_2^0(i,i) \delta S_0^2(i), \tag{38}$$

$$\bar{J}_0^2(i) \approx \bar{J}_0^{2*}(i) + \Lambda_0^2(i,i)\, \delta S_0^0(i) + \Lambda_2^2(i,i) \delta S_0^2(i), \tag{39}$$

where 'i' is the spatial grid-point under consideration, $\Lambda_0^0(i,i)$, $\Lambda_2^0(i,i)$, $\Lambda_0^2(i,i) = w^{(2)}_{J_u J_l} \Lambda_2^0(i,i)$ and $\Lambda_2^2(i,i)$ are the diagonal elements of the Λ-operators of the problem and $\delta S_0^K(i) = S_0^{K\,\mathrm{new}} - S_0^{K\,\mathrm{old}}$ (with $K = 0$ and $K = 2$). The Jacobi scheme (i.e. the local ALI method) is obtained by choosing $* =$ old in the previous expressions, while our GS-based methods are found by taking $* =$ old+new.

It is very important to understand that in typical stellar atmospheres the 'degree of anisotropy' of the radiation field is weak (i.e. $\bar{J}_0^2 / \bar{J}_0^0 \ll 1$) and that this

[10]Note that the formal solution to find I and Q at each point within the medium from given values of S_I and S_Q can be carried out applying directly the same formal solvers developed for the unpolarized case (e.g. the short-characteristics technique).

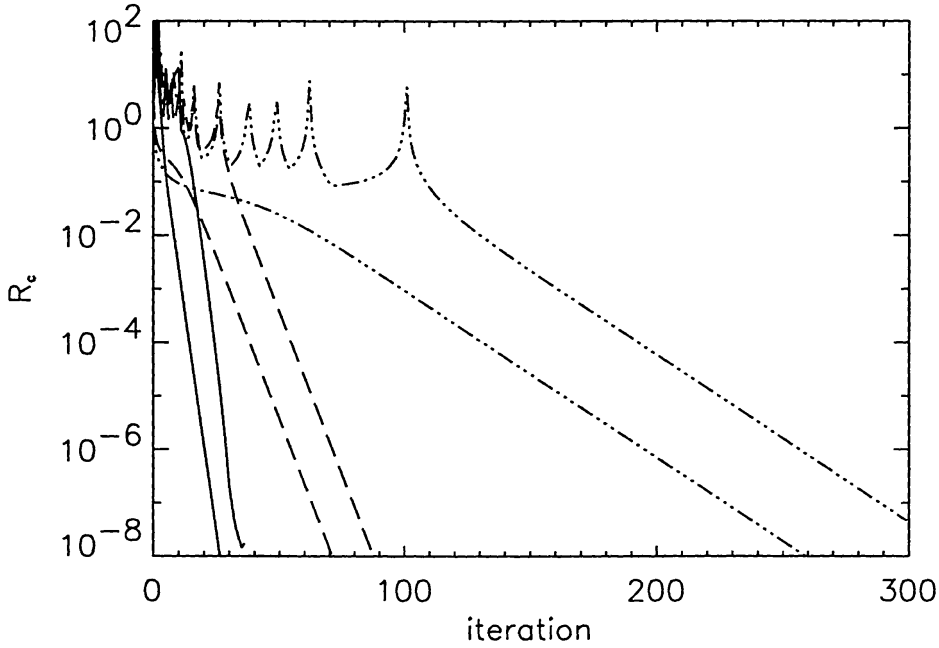

Figure 6. The maximum relative change R_c versus the iteration number for different iterative schemes. We have adopted a constant property atmosphere with collisional destruction probability $\epsilon = 10^{-4}$. Initialization: LTE values for ρ^0_0 and $\rho^2_0 = 0$. Dashed-dotted lines: the Jacobi-based ALI method. Dashed lines: the GS method. Solid lines: the SSOR method (with $\omega = 1.6$). For each pair of lines the upper one gives $R_c(\rho^2_0)$ and the lower one $R_c(\rho^0_0)$. From Trujillo Bueno & Manso Sainz (1999).

implies that the population imbalances of the J-levels are only a small fraction of their overall population (i.e. $\rho^2_0/\rho^0_0 \ll 1$). As a result, $\bar{J}^2_0$ is dominated by the Stokes I parameter (see the top panels of Fig. 6 in Trujillo Bueno 2001), which in turn is set by the S^0_0 values (i.e. by the level populations). Therefore, in most practical situations, one can simply retain the information provided by the diagonal elements of the Λ^0_0 operator and obtain the following system of equations which give the corrections at each iterative step[11]:

$$[1-(1-\epsilon)\Lambda^0_0(i,i)]\,\delta S^0_0 = (1-\epsilon)\,\bar{J}^{0*}_0 + \epsilon B_\nu - S^{0\,\mathrm{old}}_0, \tag{40}$$

$$\delta S^2_0 = \mathcal{H}\frac{(1-\epsilon)}{1+\delta(1-\epsilon)}\,w^{(2)}_{J_u J_l}\,\bar{J}^{2*}_0 - S^{2\,\mathrm{old}}_0. \tag{41}$$

Figure 6 shows an example of the convergence rate. We point out that the computing time *per iteration* is similar for the three RT methods and that matrix

[11]Note that $\bar{J}^2_0$ and S^2_0 are being improved at the rate given by Eq. (40), which yields S^0_0.

inversions are not performed at all. Thus, our pure GS method is 4 times faster than the local ALI method, while our SSOR method for polarization radiative transfer applications is 10 times faster.

Finally, it is also of interest to mention that in weakly polarizing media the Λ-iteration scheme can often be used to solve this type of resonance line polarization problems *if* one initializes using the self-consistent ρ^0_0-values corresponding to the unpolarized case (see Fig. 2 of Trujillo Bueno & Manso Sainz 1999). However, since the computing time per iteration in all these methods (Jacobi, GS, SOR and SSOR) is basically the same, it is better and safer to solve polarization transfer problems using any of our rapidly convergent iterative methods, which yield the self-consistent solution independently of the initialization.

8.2. The Hanle effect of a deterministic magnetic field

Let us now consider polarization transfer problems where the rotational symmetry of the radiation field with respect to the vertical to the stellar surface is broken[12]. This can happen either because one assumes 1D geometry with an inclined magnetic field that produces the Hanle effect, or because one is dealing with 2D or 3D geometries without any magnetic field, or because one is investigating the more general case where we have magnetic fields of any orientation in horizontally inhomogeneous stellar atmospheres. As a result, in addition to $\bar{J}^0_0$ and $\bar{J}^2_0$, we have now the real and imaginary parts of $\bar{J}^2_1$ and $\bar{J}^2_2$. These four extra radiation field tensors, which quantify the degree of breaking of the axial symmetry, are given by integrals over frequency and direction of suitable combinations of the Stokes I, Q and U parameters. We point out that, if we choose a reference system with the Z-axis along the stellar radius vector, we have $\bar{J}^0_0 \gg \bar{J}^2_0 \gg \bar{J}^2_1 \sim \bar{J}^2_2$ (e.g. Fig. 6 of Trujillo Bueno 2001).

The density-matrix elements of the upper level that are now required to fully specify the excitation state are the overall population ($\sqrt{2J_u+1}\rho^0_0(u)$), the population imbalance ($\rho^2_0(u)$), and the quantum coherences $\mathrm{Re}(\rho^2_1(u))$, $\mathrm{Im}(\rho^2_1(u))$, $\mathrm{Re}(\rho^2_2(u))$ and $\mathrm{Im}(\rho^2_2(u))$. These are the only $\rho^K_Q(u)$ elements that can be different from zero, independently of the J_u value. This is a consequence of the assumption of *unpolarized ground level* and of the fact that the radiation field tensor $\bar{J}^K_Q$ only has $K \leq 2$. In fact, if we allowed for the possibility of ground-level polarization (e.g. $\rho^K_0(l) \neq 0$ with K even) then the absorption of the $K=2$ component of the radiation field tensor could generate non-zero ρ^{K+2}_0 values (see section 9).

When studying Hanle-effect problems like the one we are considering here it is interesting to write the SE equations in a reference system with the quantization axis of total angular momentum chosen along the vertical. In this case, Eq. (15) is still valid, except that the magnetic term (i.e. the first term of the *rhs*) becomes equal to $-2\pi i \nu_L\, g_J \sum_{Q'} \mathcal{K}^K_{QQ'} \rho^K_{Q'}(J)$, where $\mathcal{K}^K_{QQ'}$ is a magnetic kernel which couples the density matrix elements of given rank K among themselves

[12] See also the information provided by Nagendra (2002) concerning their formulation of the two-level atom Hanle-effect problem without ground level polarization, but taking into account PRD effects. For additional information see Faurobert-Scholl, Frisch & Nagendra (1997), and Paletou & Faurobert-Scholl (1997).

(Landi Degl'Innocenti, Bommier and Sahal-Bréchot 1990). The application of the general SE equations to the present two-level atom problem still yields expression (31) for S^0_0, but the following five equations for S^2_Q (see Manso Sainz & Trujillo Bueno 1999):

$$[1+\delta(1-\epsilon)]\begin{pmatrix} S^2_0 \\ \tilde{S}^2_1 \\ \hat{S}^2_1 \\ \tilde{S}^2_2 \\ \hat{S}^2_2 \end{pmatrix} = -(1-\epsilon)\Gamma_u \begin{pmatrix} 0 & M_{12} & M_{13} & M_{14} & M_{15} \\ M_{21} & 0 & M_{23} & M_{24} & M_{25} \\ M_{31} & M_{32} & 0 & M_{34} & M_{35} \\ M_{41} & M_{42} & M_{43} & 0 & M_{45} \\ M_{51} & M_{52} & M_{53} & M_{54} & 0 \end{pmatrix} \begin{pmatrix} S^2_0 \\ \tilde{S}^2_1 \\ \hat{S}^2_1 \\ \tilde{S}^2_2 \\ \hat{S}^2_2 \end{pmatrix} + (1-\epsilon)\, w^{(2)}_{J_u J_l} \begin{pmatrix} \bar{J}^2_0 \\ \tilde{J}^2_1 \\ -\hat{J}^2_1 \\ \tilde{J}^2_2 \\ -\hat{J}^2_2 \end{pmatrix}, \tag{42}$$

with $\Gamma_u = 8.79 \times 10^6 g_{J_u} B/A_{ul}$ (with B in gauss and A_{ul} in s^{-1}), and where $\tilde{S}^2_Q$ and $\tilde{J}^2_Q$ indicate the *real* parts, while $\hat{S}^2_Q$ and $\hat{J}^2_Q$ the *imaginary* parts. The M_{ij}-coefficients, which can be obtained from the components of the magnetic kernel $\mathcal{K}$, depend on the orientation of the local magnetic field vector (see Table 1 of Landi Degl'Innocenti et al. 1990). The SE equations (42) have a clear physical meaning. The magnetic operator $\mathcal{M}$ couples locally the $K = 2$ statistical tensors among them. The second term in the *r.h.s.* of Eq. (42) is the radiative coupling term. It 'transfer' the symmetry properties of the radiation field *directly* to the atomic system. Therefore, even if $\Gamma_u = 0$ optical pumping processes can generate both *population imbalances* (if $\bar{J}^2_0 \neq 0$) and *coherences* (if $\bar{J}^2_1 \neq 0$ and/or $\bar{J}^2_2 \neq 0$). In the presence of an inclined field such S^2_Q values are modified by the action of the magnetic operator (the Hanle effect). On the other hand, assuming $\bar{J}^2_1 = \bar{J}^2_2 = 0$ all coherences are zero if $\Gamma_u = 0$. However, in the presence of an inclined magnetic field (but still assuming $\bar{J}^2_1 = \bar{J}^2_2 = 0$ on the basis of the argument that in stellar atmospheres they are much smaller than $\bar{J}^K_0$) *coherences* are generated through the magnetic operator. As deduced from Eq. (42), this is possible thanks to the *population imbalances* (S^2_0) that are directly induced by the anisotropic illumination ($\bar{J}^2_0$). In *magnetized* stellar atmospheres, the population imbalances themselves are in fact the main 'source' of quantum coherences (i.e. from the point of view of the above-mentioned reference system).

The transfer equations for this type of Hanle-effect problems where the ground level is assumed to be unpolarized are similar to Eqs. (34) and (35), but with an extra equation for the Stokes U-parameter. As shown in detail by Manso Sainz & Trujillo Bueno (1999), the iterative methods of section 3 can be obtained easily by introducing into the previous SE equations the following approximations:

$$\begin{aligned} \bar{J}^0_0(i) &\approx \bar{J}^{0\,*}_0(i) + \Lambda^0_0(i,i)\delta S^0_0(i)\,, \\ \bar{J}^2_Q(i) &\approx \bar{J}^{2\,*}_Q(i), \end{aligned} \tag{43}$$

where $*$ = old for Jacobi and $*$ = old+new for the Gauss-Seidel scheme, being 'i' the spatial grid-point under consideration. One then obtains, at each grid-point 'i' independently, a system of equations that can be solved easily to find the *new* values of $S^K_Q(i)$. We point out that this is equivalent to applying the operator splitting technique to the Λ^0_0 operator only. It can be demonstrated that in stellar atmospheres no gain is obtained if the splitting is applied to the whole set of 36 operators that correspond to this Hanle-effect problem (Manso Sainz & Trujillo Bueno 1999).

All these equations are valid in 1D, 2D and 3D. The only difference is the formal solver that one has to apply in each case. Thus, for example, for 2D Hanle-effect problems with horizontal periodic boundary conditions a very suitable 2D formal solution technique is that developed by Auer, Fabiani Bendicho and Trujillo Bueno (1994), while for solving the Hanle effect problem in 3D we use the formal solver developed by Fabiani Bendicho & Trujillo Bueno (1999).

8.3. Non-LTE Zeeman line transfer

Finally, we consider the case of Zeeman line transfer for situations where the magnetic field is sufficiently strong (typically $B > 100$ Gauss) so that the Zeeman splitting of the atomic levels is much larger than the natural width. This implies that *in the magnetic field reference frame* all the quantum coherences between the Zeeman sublevels vanish, which means that only the ρ^K_Q elements with Q=0 suffice to describe the atomic excitation (Landi Degl'Innocenti, Bommier and Sahal-Bréchot 1991). Since we now have Zeeman splitting with magneto-optical effects, all the coefficients of the absorption matrix $\mathbf{K}$ are in principle non-zero and the solution of this problem requires the application of a fast an accurate formal solver of the Stokes-vector transfer equation. To this end, a good choice is to apply the DELOPAR method described in section 6. One should distinguish two cases:

(1) Zeeman line transfer without atomic level polarization. With this simplification, the unknowns of the problem are the same as those corresponding to the standard Non-LTE problem, i.e. the overall population of each atomic level ($\sqrt{2J+1}\rho^0_0$). The only novelty is that, in the SE equations, instead of having for each radiative transition the well-known quantity $\bar{J}$ (which is identical to the radiation field tensor $\bar{J}^0_0$), we have

$$\bar{J}_{\rm pol} = \frac{1}{4\pi} \int {\rm d}x \int {\rm d}\vec{\Omega} \, [\, \Phi_I \, I \, + \, \Phi_Q \, Q \, + \, \Phi_U \, U \, + \, \Phi_V \, V \,] \,, \qquad (44)$$

where Φ_X (with $X = I, Q, U$ or V) are the profiles of the first row (or column) of the 4×4 line absorption matrix, which depend on the Zeeman splitting and on the direction of the magnetic field vector with respect to the direction $\vec{\Omega}$ of each ray. Therefore, the numerical solution of the multilevel Zeeman line transfer problem *without* atomic polarization can be carried out applying directly any of the operator splitting methods of section 3. For instance, for the case of a two-level atomic model the relevant equation to be solved iteratively is

$$S = (1 - \epsilon) \, \bar{J}_{\rm pol} \, + \, \epsilon \, {\rm B}_\nu , \qquad (45)$$

It is straightforward to show that the application of the iterative schemes of section 3 yields an iterative correction similar to Eq. (8) for the local ALI method, and to Eq. (10) for our GS-based schemes[13]. The only difference is that now we need to calculate $\bar{J}_{\rm pol}$ and the diagonal elements of the Λ operator of the problem, whose values depend on the Zeeman splitting. The resulting convergence rate is similar to that shown in Fig. 6 for the ρ^0_0 values. Some interesting model calculations have been presented by Trujillo Bueno & Landi Degl'Innocenti (1996) and by Bruls & Trujillo Bueno (1996). These authors investigated in detail the impact of the Zeeman splitting on the atomic level populations in the presence of magnetic field gradients. Previously, such an impact had been investigated for constant magnetic fields only (Rees 1969; Domke & Staude 1973; Auer, Heasley & House 1977). Of particular interest is the 'polarization-free' approximation of Trujillo Bueno & Landi Degl'Innocenti (1996), i.e. $\bar{J}_{\rm pol} \approx \frac{1}{4\pi} \int {\rm d}x \int {\rm d}\vec{\Omega}\, \Phi_I\, I$, which provides a fairly good account of the effects of homogeneous and inhomogeneous magnetic fields on the statistical equilibrium without having to solve the Stokes-vector transfer equation[14].

(2) Zeeman line transfer with atomic level polarization. Considering atomic polarization in the Zeeman line transfer problem complicates the situation considerably. First, the number of unknowns grows significantly, since one must calculate the population of each Zeeman sublevel (or, alternatively, the ρ^K_0 density matrix elements). Second, there is no longer a single radiation field tensor that plays a role in the SE equations. In principle, we may have both atomic *orientation* (e.g. ρ^1_0) and *alignment* (e.g. ρ^2_0).

One has atomic orientation in a given level when the populations of its Zeeman sublevels with magnetic quantum numbers M and $-M$ are different. In the absence of level crossings between the J-levels (or between the F-levels if we were dealing with a hyperfine structured multiplet) the only way to induce atomic orientation is via a radiation field showing *net* circular polarization *or* if the pumping radiation has *spectral structure* over a frequency interval $\Delta\nu$ smaller than the frequency separation between the Zeeman sublevels (e.g. via Doppler-shifted spectral-line radiation). Although solar-like atmospheres have both magnetic fields and macroscopic mass motions, there is a physical argument that suggests that the errors we make by neglecting atomic orientation might be small. This is because the level populations in realistic atomic models are controlled mainly by strong UV line transitions and continua. The critical UV lines are broad and weakly split.

The other manifestation of atomic level polarization is *alignment*, which is non-zero when states of different $|M|$ are unequally populated, while the populations in M and $-M$ can be the same. This can simply occur via anisotropic radiation pumping, even in the presence of the Zeeman splitting of a strong magnetic field. However, from the two-level atom calculations of Bommier & Landi Degl'Innocenti (1996), we expect the influence of atomic alignment on the emergent Stokes profiles to be significant mainly for weakly split lines and concerning only Q and U. Bommier & Landi Degl'Innocenti (1996) applied nu-

[13]See also Takeda's (1991) alternative formulation of the local ALI method.

[14]Note that the profile Φ_I accounts for the Zeeman broadening of the Stokes I profile.

merical methods that require the construction and inversion of large matrices. Fortunately, this type of problems (including its generalization to the full multilevel case) can be solved in a much more efficient and general way applying the iterative methods discussed in section 3. To this end, it suffices to follow the same ideas that we have summarized above. Finally, it may be useful to mention that Sánchez Almeida & Trujillo Bueno (1999) introduced a suitable approximation for facilitating the numerical solution of the general Zeeman line transfer problem. Figure 7 of their paper illustrates that sizable population imbalances can indeed be generated even in the presence of relatively strong fields.

9. Non-linear Problems: taking into account lower-level polarization

The assumption of unpolarized lower-level is strictly true for line transitions with J_l=0 of atoms without hyperfine structure[15]. The argument used in favour of this simplifying approximation for other J_l values is that the lower level of a line transition is generally long-lived, and that it must thus have plenty of time to be depolarized by elastic collisions and/or weak magnetic fields (Stenflo, 1994). However, it has been demonstrated recently that the *ground* and *metastable* levels of a variety of solar spectral lines are indeed significantly polarized (see the review by Trujillo Bueno 2001).

The consideration of lower-level atomic polarization leads to a coupled system of *non-linear* equations, even for the case of a two-level model atom. Moreover, it implies that even in the unmagnetized case the absorption matrix $\mathbf{K}$ is *not* simply given by $\eta_I \mathbf{1}$. As a result, there is always a coupling of the intensity with the Stokes Q and U parameters which is due to the absorption process. In other words, now we have *dichroism*, i.e. the absorption coefficient in the line transition depends on the polarization of the incident radiation.

9.1. Multilevel scattering polarization without magnetic fields

Let us consider first the 1D case of a plane-parallel atmosphere without magnetic fields. As in section 8.1 the symmetry properties of the radiation field are described by $\bar{J}^0_0$ and $\bar{J}^2_0$ and there are no coherences. Moreover, the only non-zero Stokes parameters are I and Q, and the Stokes-vector transfer equation (21) reduces to

$$\frac{d}{ds} I = \epsilon_I - \eta_I \, I - \eta_Q \, Q, \tag{46}$$

$$\frac{d}{ds} Q = \epsilon_Q - \eta_Q \, I - \eta_I \, Q, \tag{47}$$

where the emission and absorption coefficients are given by expressions (28) and (29), but with $\rho^2_1 = \rho^2_2 = 0$.

It is easy to show from these equations that the emergent fractional polarization at μ is approximately given by (Trujillo Bueno 1999; 2001):

[15]Note also that a level with $J = 1/2$ can be *oriented* but not *aligned*.

$$Q/I \approx \frac{3}{2\sqrt{2}}(1-\mu^2)[\mathcal{W}\,\sigma_0^2(\mathrm{up}) - \mathcal{Z}\,\sigma_0^2(\mathrm{low})], \tag{48}$$

where the reference direction for $Q > 0$ has been chosen here along the line perpendicular to the radial direction through the observed point. We note that $\sigma_0^2 = \rho_0^2/\rho_0^0$ (i.e. it is the fractional atomic alignment), while $\mathcal{W} = w^{(2)}_{J_u J_l}$ and $\mathcal{Z} = w^{(2)}_{J_l J_u}$ (e.g. $\mathcal{W} = \mathcal{Z} = -1/2$ for a transition with $J_l = J_u = 1$). In Eq. (48) the σ_0^2 values are those corresponding to the optical depth τ where $\tau/\mu \approx 1$ (which means $\tau = 0$ for a limb observation at $\mu = 0$). Formula (48) shows that the observed linear polarization amplitude in a given spectral line has in general two contributions: one from the fractional alignment of the upper-level ($\sigma_0^2(u)$) and an extra one from the fractional alignment of the lower level ($\sigma_0^2(l)$). In general, the first contribution (caused exclusively by the emission events from the polarized upper level) is the only one that is normally taken into account. However, the second contribution (caused by the selective absorption resulting from the population imbalances of the lower level) plays the key role in producing the 'enigmatic' linear polarization signals that have been discovered recently in 'quiet' regions close to the solar limb[16], as well as in solar filaments (Trujillo Bueno 1999, 2001; Manso Sainz & Trujillo Bueno 2001; Trujillo Bueno et al. 2002*b*; see also Trujillo Bueno & Landi Degl'Innocenti 1997).

The formal solution of the transfer equations (46) and (47) can be carried out using any of the methods previously developed for the unpolarized case. This is because, in place of Eqs. (46) and (47), one can write two decoupled transfer equations: one for $I^+ = I + Q$ (with absorption coefficient $\eta^+ = \eta_I + \eta_Q$ and emission coefficient $\epsilon^+ = \epsilon_I + \epsilon_Q$) and an extra one for $I^- = I - Q$ (with absorption coefficient $\eta^- = \eta_I - \eta_Q$ and emission coefficient $\epsilon^- = \epsilon_I - \epsilon_Q$).

The SE equations are given by Eq. (15), but without the magnetic term because here $\nu_L = 0$. As mentioned above, the only non-zero radiation field tensors are $\bar{J}^0_0$ (intensity) and $\bar{J}^2_0$ (anisotropy). As a result, each level of total angular momentum J is described by its *overall population* ($\sqrt{2J+1}\rho^0_0$) and by a hierarchy of *population imbalances* quantified by[17] ρ^2_0, ρ^4_0, ρ^6_0, ... $\rho^{K_{\max}}_0$, whose absolute values decrease with increasing K. Note that we can now induce ρ^K_0 values with $K = 4, 6, ..., K_{\max}$ because the lower levels of the line transitions of the assumed atomic model can be polarized.

The best we can do to illustrate the additional complexity is to apply the general equations (15) to the case of a gas of two-level atoms with $J_l = J_u = 1$, neglecting stimulated emission processes, but taking fully into account the possibility of atomic polarization in both levels (Trujillo Bueno 1999). We obtain

$$\frac{d}{dt}\rho^0_0(u) = B_{lu}\,[\bar{J}^0_0\rho^0_0(l) - \frac{\bar{J}^2_0\rho^2_0(l)}{2}] - A_{ul}\rho^0_0(u) \tag{49}$$
$$+C_{lu}\rho^0_0(l) - C_{ul}\rho^0_0(u) = 0\,,$$

[16]See the observations of Stenflo, Keller & Gandorfer (2000).

[17]Since $K_{\max} = 2J$ for integer values of J and $K_{\max} = 2J-1$ for half-integer values of J, the total number of $\rho^K_0(J)$ elements is $J+1$ and $J+1/2$, respectively.

$$\frac{d}{dt}\rho^2_0(u) = -\left[\frac{B_{lu}}{2}\bar{J}^2_0\rho^0_0(l) + \frac{B_{lu}}{2}\bar{J}^0_0\rho^2_0(l) + \frac{B_{lu}}{\sqrt{2}}\bar{J}^2_0\rho^2_0(l)\right] - A_{ul}\,\rho^2_0(u) \qquad (50)$$
$$+C^{(2)}_{lu}\rho^2_0(l) - (C_{ul} + D^{(2)}(u))\rho^2_0(u) = 0\,,$$

$$\frac{d}{dt}\rho^2_0(l) = -A_{ul}\rho^2_0(u) + \left[B_{lu}\bar{J}^2_0\rho^0_0(l) - 2B_{lu}\bar{J}^0_0\rho^2_0(l) - \frac{B_{lu}}{\sqrt{2}}\bar{J}^2_0\rho^2_0(l)\right] \qquad (51)$$
$$+2\,C^{(2)}_{ul}\rho^2_0(u) - 2(C_{lu} + D^{(2)}(l))\rho^2_0(l) = 0\,,$$

$$\rho^0_0(l) + \rho^0_0(u) = 1/\sqrt{3}\,, \qquad (52)$$

where the last equation expresses the conservation of the number of particles.

The number of unknowns is only four (i.e. $\rho^0_0(u), \rho^2_0(u), \rho^0_0(l)$, and $\rho^2_0(l)$). However, this is only because we are considering the illustrative example of a two-level atom with $J_l = J_u = 1$. In fact, the mere presence of lower-level polarization implies that we have to solve a *non-local* and *non-linear* RT problem of exactly the same nature as the general *Non-LTE problem of the* 2^{nd} *kind.* The non-linearity is caused by the terms of the form $\bar{J}^K_Q\rho^k_q$. To solve the general multilevel problem we have developed the methods **DALI** and **DEGAS** summarized below (see Trujillo Bueno 1999).

With **DALI** and **DEGAS** everything goes as simply as in the Λ-iteration scheme, but the convergence rate is *extremely* high (see an example in Fig. 7). **DALI**, besides the name of the famous Spanish painter, is an acronym for Density-matrix ALI method (which is based on Jacobi iteration), while **DEGAS**, besides the name of the fine French painter, refers here to my Density-matrix Gauss-Seidel iterative scheme. The basic idea, inspired by the preconditioning approach of Rybicki & Hummer (1991; 1992), consists in making the following changes for achieving linearity in the SE equations at each iterative step:

If K≠0,

$$\bar{J}^K_Q\ \rho^k_q \ \rightarrow\ \bar{J}^{K*}_Q\ \rho^{k^{new}}_q \qquad (53)$$

If K=0,

$$\bar{J}^0_0\ \rho^k_q \ \rightarrow\ \bar{J}^{0*}_0\ \rho^{k^{new}}_q + \Lambda^0_0(i,i)\,[\,\rho^{k^{old}}_q\rho^{0^{new}}_0(u) - \rho^{0^{old}}_0(u)\,\rho^{k^{new}}_q\,], \qquad (54)$$

where $\Lambda^0_0(i,i)$ ('i' being the spatial grid-point under consideration) is the *diagonal* element of the Λ^0_0 operator that arises in the definition of $\bar{J}^0_0$, and where '*old*' means to take the value of the previous iterative step, while '*new*' indicates the improved values of the density-matrix elements that are to be obtained at

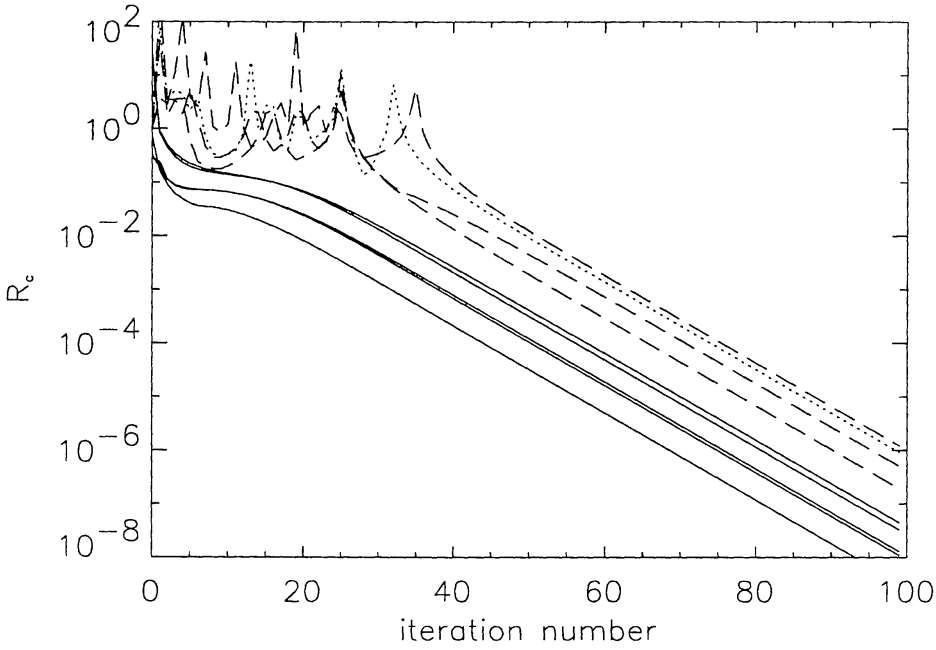

Figure 7. The convergence rate of the DALI method when solving the multilevel scattering polarization problem assuming a 5-level Ca II model (with the H & K resonance lines and the IR triplet) and a semi-empirical model of the solar chromosphere. Initialization: LTE values for ρ^0_0 and $\rho^K_0 = 0$. The number of ρ^K_0 elements is 9 at each spatial grid point. We would have 29 ρ^K_Q elements in the presence of a deterministic magnetic field, which is the case of Fig. 8.

the current iterative step by simply solving the resulting linear system of equations. In the DALI method we take $* =$ old, while with DEGAS we have $* =$ old+new, with the ensuing radiation field tensors (and also $\Lambda^0_0(i,i)$) calculated, at each iterative step, as explained in section 3 (see also Trujillo Bueno and Manso Sainz, 1999). For the solution of scattering line polarization problems using realistic multilevel atoms it is better to initialize the calculation using the ρ^0_0 self-consistent values corresponding to the *unpolarized* case. With this initialization given, it is easy to obtain rapidly the self-consistent solution of any Non-LTE problem of the 2^{nd} kind applying either DALI iteration or DEGAS iteration.

9.2. Multilevel scattering polarization in the presence of weak magnetic fields

Finally, we turn our attention to consider the multilevel problem of the Hanle and Zeeman effects acting together in weakly magnetized stellar atmospheres (e.g. with $B \leq 100$ G). In this range of magnetic field strengths the Zeeman splitting is typically a very small fraction of the spectral line width, and the contribution of the *transverse* Zeeman effect to the emergent linear polarization

is negligible. Therefore, we are considering here a regime in which the linear polarization signatures are governed by scattering processes and the Hanle effect, while the circular polarization is the result of the longitudinal Zeeman effect. Obviously, in this more complicated case all four Stokes parameters come into play. However, since in weakly magnetized stellar atmospheres $\epsilon_I \gg \epsilon_Q, \epsilon_U, \epsilon_V$ and $\eta_I \gg \eta_Q, \eta_U, \eta_V, \rho_Q, \rho_U, \rho_V$, (which in turn implies that $I \gg Q, U, V$) the Stokes-vector transfer equation (21) simplifies to

$$\frac{d}{ds} I = \epsilon_I - \eta_I \, I - \eta_Q \, Q - \eta_U \, U - \eta_V \, V \approx \epsilon_I - \eta_I \, I, \tag{55}$$

$$\frac{d}{ds} Q \approx \epsilon_Q - \eta_Q \, I - \eta_I \, Q, \tag{56}$$

$$\frac{d}{ds} U \approx \epsilon_U - \eta_U \, I - \eta_I \, U, \tag{57}$$

$$\frac{d}{ds} V \approx \epsilon_V - \eta_V \, I - \eta_I \, V. \tag{58}$$

In these transfer equations the Stokes I, Q and U components of the emission vector and absorption matrix are given by Eqs. (28)-(30), while ϵ_V and η_V include only the contribution of the longitudinal Zeeman effect.

The formal solution can be carried out efficiently applying the DELOPAR method outlined in section 6. For each radiative transition the formal solver calculates the diagonal elements of the Λ^0_0 operator and six radiation field tensors ($\bar{J}^0_0$, $\bar{J}^2_0$, and the real and imaginary parts of $\bar{J}^2_1$ and $\bar{J}^2_2$). The numerical calculation is harder now because we have to discretize not only the polar angle (to specify the inclination of each radiation beam) but also the azimuthal angle [18]. We formulate the statistical equilibrium Eqs. (15) using a reference system with the quantization axis along the vertical. Therefore, we have again the action of the magnetic operator of section 8.2, which produces a local coupling of all the ρ^K_Q elements of the same rank K, but now for each of the levels of the assumed multilevel atom.

Finally, note that the total number of ρ^K_Q unknowns associated to each level of total angular momentum value J is $(J+1)(2J+1)$ (for J integer) and $J(2J+1)$ (for J half-integer). The numerical solution of the *non-local* and *non-linear* sets of equations can be carried out efficiently applying the same DALI and DEGAS methods outlined above. In fact, Manso Sainz & Trujillo Bueno (2002) have successfully developed a general multilevel program for the numerical simulation of the Hanle and Zeeman effects in weakly magnetized stellar atmospheres. Figure 8 shows an example of a numerical simulation of the Hanle and Zeeman effects, which explains the four Stokes profiles of the 'enigmatic' Ca II 8662 Å line that we have observed in weakly magnetized regions of the solar chromosphere at $\mu = 0.1$. Of particular interest are the Stokes Q and U profiles, whose physical origin is the existence of *population imbalances* and *coherences* in the metastable lower-level.

[18] This is necessary now, even for the 1D case, because of the presence of lower-level atomic polarization (Manso Sainz & Trujillo Bueno 2002).

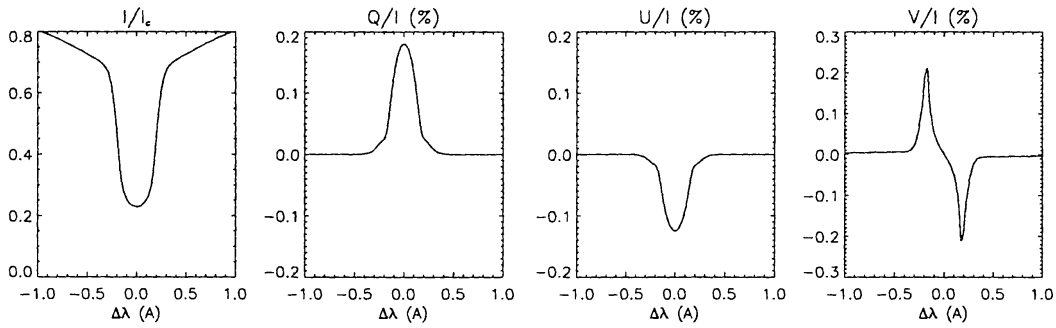

Figure 8. The emergent Stokes parameters of the Ca II 8662 Å line calculated at $\mu = 0.1$ in a semi-empirical model of the solar atmosphere. We have assumed a magnetic field of 20 gauss that is inclined by 25° with respect to the radial direction. This RT modeling yields a fairly good fit to the spectropolarimetric observation of the Ca II 8662 Å line shown in Trujillo Bueno & Manso Sainz (2002).

10. Concluding remarks

The modeling of spectral line polarization in stellar atmospheres should be done applying a rigorous theory for the generation and transfer of polarized radiation. The quantum theory of line formation provides a robust and suitable framework for the investigation of polarization transfer problems aimed at a confrontation with high-sensitivity spectro-polarimetric observations. Although it is indeed a complicated QED theory, it is worthwhile the effort to study it in detail because it allows us to formulate with confidence RT problems of increasing complication, taking properly into account a variety of subtle physical mechanisms that play a key role in producing the observed polarization signals.

Besides providing an introduction to the quantum theory of polarization, the main aim of this article has been to show that the ensuing statistical equilibrium and Stokes-vector transfer equations can be solved efficiently with the same iterative methods and formal solvers we had previously developed for the fast and accurate solution of RT problems in one, two and three-dimensional geometries.

Acknowledgments. I would like to thank Andrés Asensio Ramos, Peña Fabiani Bendicho, Rafael Manso Sainz and Héctor Socas-Navarro for stimulating discussions on radiative transfer and spectropolarimetry. This work has been partly funded by the Spanish Ministerio de Ciencia y Tecnología through project AYA2001-1649.

References

Auer, L.H., Heasley, J.N. & House, L.L. 1977, ApJ, 216, 531

Auer, L.H., Fabiani Bendicho, P. & Trujillo Bueno, J. 1994, A&A, 292, 599

Bommier, V. 1997 a, A&A, 328, 706

Bommier, V. 1997 b, A&A, 328, 726

Bommier, V., & Sahal-Bréchot, S. 1978, A&A, 69, 57

Bommier, V. & Landi Degl'Innocenti, E. 1996, Sol. Phys., 164, 117

Born, M., & Wolf, E. 1994, *Principles of Optics*, Pergamon Press, Oxford

Brink, D.M. & Satchler, G.R. 1968, *Angular Momentum*, Clarendon Press, Oxford

Bruls, J.H.M.J. & Trujillo Bueno, J. 1996, Sol. Phys., 164, 155

Domke, H. & Staude, J. 1973, Sol. Phys., 31, 279

Fabiani Bendicho, P., Trujillo Bueno, J. & Auer, L.H. 1997, A&A, 324, 161

Fabiani Bendicho, P., & Trujillo Bueno, J. 1999, '3D Radiative Transfer with Multilevel Atoms', in *Solar Polarization*, K. N. Nagendra & J. O. Stenflo (eds.), Kluwer Academic Publishers, 219-230

Fano, U. 1957, Rev. Mod. Phys., 29, 74

Faurobert-Scholl, M., Frisch, H. & Nagendra, K.N. 1997, A&A, 322, 896

Hageman, L.A. & Young, D.M. 1981, *Applied Iterative Methods*, Academic Press, New York

Hanle, W. 1924, Z. Phys., 30, 93

Kastler, A. 1950, J. de Physique, 11, 255

Kunasz, P. & Auer, L.H. 1988, J. Quant. Spectrosc. Radiat. Transfer, 39, 67

Lamb, F.K. & Ter Haar, D. 1971, Physics Reports, 2C(4), 253

Landi Degl'Innocenti, E. 1983, Sol. Phys., 85, 3

Landi Degl'Innocenti, E. 1984, Sol. Phys., 91, 1

Landi Degl'Innocenti, E. 1985, Sol. Phys., 102, 1

Landi Degl'Innocenti, E. 1992, in *Solar Observations: Techniques and Interpretation*, F. Sánchez, M. Collados and M. Vázquez (eds.), Cambridge University Press, 73

Landi Degl'Innocenti, E. 2002, in *Astrophysical Spectropolarimetry*, J. Trujillo Bueno, F. Moreno-Insertis & F. Sánchez (eds.), Cambridge University Press, 1

Landi Degl'Innocenti, E. & Landi Degl'Innocenti, M. 1985, Sol. Phys., 97, 239

Landi Degl'Innocenti, E., Bommier, V. & Sahal Bréchot, S. 1990, A&A, 235, 459

Landi Degl'Innocenti, E., Bommier, V. & Sahal Bréchot, S. 1991, A&A, 244, 401

Landi Degl'Innocenti, E., Landi Degl'Innocenti, M., & Landolfi, M. 1997, in *Science with THEMIS*, N. Mein and Sahal-Bréchot, S. (eds.), Paris Obs. Publ., p. 59

Manso Sainz, R., & Trujillo Bueno, J. 1999, 'The Hanle Effect in 1D, 2D and 3D', in *Solar Polarization*, K. N. Nagendra & J. O. Stenflo (eds.), Kluwer, 143-156

Manso Sainz, R., & Trujillo Bueno, J. 2001, 'Modeling the Scattering Line Polarization in the Ca II IR Triplet', in *Advanced Solar Polarimetry*, M. Sigwarth (ed.), ASP Conf. Series, Vol. 236, 213-220.

Manso Sainz, R., & Trujillo Bueno, J. 2002, (in preparation)

Mihalas, D. 1978, *Stellar Atmospheres*, Freeman

Nagendra, K.N. 2002 (this volume)

Olson, G.L., Auer, L.H. & Buchler, J.R. 1986, J. Quant. Spectrosc. Radiat. Transfer, 35, 431

Omont, A. 1977, Prog. Quantum Electron., 5, 69

Paletou, F. & Faurobert-Scholl, M. 1997, A&A, 328, 343

Rees, D.E. 1960, Sol. Phys., 10, 268

Rees, D.E., Murphy, G.A. & Durrant, C.J. 1989, ApJ, 339, 1093

Rybicki, G.B. & Lightman, A.P. 1979, *Radiative Processes in Astrophysics*, John Wiley & Sons, New York

Rybicki, G.B. & Hummer, D.G. 1991, A&A, 245, 171

Rybicki, G.B. & Hummer, D.G. 1992, A&A, 262, 209

Sánchez Almeida, J., & Trujillo Bueno, J. 1999, ApJ, 526, 1013

Shchukina, N. & Trujillo Bueno, J. 2001, ApJ, 550, 970

Socas-Navarro, H. & Trujillo Bueno, J. 1997, ApJ, 490, 383

Socas-Navarro, H. Trujillo Bueno, J. & Ruiz Cobo, B. 2000a, ApJ, 530, 977

Socas-Navarro, H. Trujillo Bueno, J. & Ruiz Cobo, B. 2000b, Science, 288, 1396

Stenflo, J.O. 1994, *Solar Magnetic Fields: Polarized Radiation Diagnostics*, Kluwer Academic Publishers

Stenflo, J.O., Keller, C., & Gandorfer, A. 2000, A&A, 355, 789

Takeda, Y. 1991, Publ. Astron. Soc. Japan., 43, 719

Trujillo Bueno, J. 1990, 'Radiative Transfer Problems in Solar-like Atmospheres', in *New Windows to the Universe*, Vol. 1, F. Sánchez & Vázquez (eds.), Cambridge University Press, 119-160

Trujillo Bueno, J. 1999, 'Towards the Modeling of the Second Solar Spectrum', in *Solar Polarization*, K. N. Nagendra & J. O. Stenflo (eds.), Kluwer Academic Publishers, 73-96

Trujillo Bueno, J. 2001, 'Atomic Polarization and the Hanle Effect', in *Advanced Solar Polarimetry: Theory, Observation and Instrumentation*, M. Sigwarth (ed.), ASP Conf. Series, Vol. 236, 161-195

Trujillo Bueno, J. 2002, (in preparation)

Trujillo Bueno, J. & Fabiani Bendicho, P. 1995, ApJ, 455, 646

Trujillo Bueno, J. & Landi Degl'Innocenti, E. 1996, Sol. Phys., 164, 135

Trujillo Bueno, J. & Landi Degl'Innocenti, E. 1997, ApJ Letters, 482, L183

Trujillo Bueno, J. & Manso Sainz, R. 1999, ApJ, 516, 436

Trujillo Bueno, J. & Manso Sainz, R. 2002, Il Nuovo Cimento C, Vol. 25, (in press)

Trujillo Bueno, J., Moreno Insertis, F., & Sánchez, F. (eds.) 2002*a*, *Astrophysical Spectropolarimetry*, Cambridge University Press

Trujillo Bueno, J. & Landi Degl'Innocenti, E., Collados, M., Merenda, L. & Manso Sainz, R. 2002*b*, Nature, 415, 403